Controlling Polymorphism in Pharmaceutical Compounds Using Solution Shearing

A Thesis Presented to

The Faculty of the School of Engineering and Applied Science

University of Virginia

In partial fulfillment of the requirements for the degree of

Master of Science

By Stephanie Guthrie

November 2017

ACKNOWLEDGEMENT

Contents

List of Figures

Figure 1. Development of a single FDA approved drug begins with several thousand candidate molecules.

Figure 2. a) Two crystal forms of the same material have different solubilities. Reprinted with permission from Kim, J.-W.; *Cryst. Growth. Des.* **2012,** *12* (10), 4739-4744. Copyright 2017. American Chemical Society. b) Amorphous and metastable crystal forms display enhanced dissolution kinetics. Adapted from Brittain, H., *Am Pharmaceut Rev* **2014,** *17* (3), 10-6.

Figure 3. Different solid states form through assembly of the same base molecule in different ways. Amorphous materials have no long-range order associated with molecular arrangement. Polymorphs have ordered unit cells with dissimilar molecular packing that creates different unit cell shapes and sizes.

Figure 4. Crystallization is an energetic event with intermediate crystal forms existing. Prior to arriving at the most thermodynamically stable crystal, a drug may pass through kinetic crystal forms that are metastable.

Figure 5. Traditionally, the parameters of temperature, concentration and solvent selection are extensively used to influence the supersaturation of a system. Through this the nucleation and growth regimes are selected for desired crystallization behavior.

Figure 6. In solution shearing, changing the blade speed optimizes device performance through a) changing the shape and size of the unit cell (d-spacing) and b) increasing charge transport as a result of polymorphism. Figure used with permission from Giri, G. *Nature* **2011,** *480* (7378), 504-508.

Figure 7. Molecular structure a) glycine and b) acetaminophen used in this study.

Figure 8. Using cross-polarized optical microscopy, crystal alignment can be studied. Similarly aligned domains have similar intensities as samples are rotated.

Figure 9: a) Schematic of diffraction measurements taken parallel and perpendicular to the blade direction. b) Characteristic film morphologies and corresponding GIXD patterns relevant to this work.

Figure 10. (a) Conceptual image of the solution shearing technique for thin film formation. (b) Evaporative and Landau-Levich shearing regimes. In the evaporative regime, film thickness decreases as shearing speed increases ($h \propto v^{-1}$). In the Landau-Levich regime, film thickness increases with shearing speed, ($h \propto v^{2/3}$). Trendlines adapted from equations outlined by Le Berre et al. with parameters updated to reflect the water-pharmaceutical system in this study.

Figure 11. (a) Film thickness data overlaid on theoretical evaporative regime trendline. Thickness measurements of glycine at (b) 70 ˚C with exponential factor of -0.93 and (c) 100 ˚C with exponential factor of -1.28. Exponential factors, suggest operation in the evaporative regime.

Figure 12. Glycine and acetaminophen thin films formed at a range of blade speeds, at. Films imaged at 20x, scale bar is 20 μm, and sample orientation relative to shearing direction is indicated with arrow.

Figure 13. Film rotation shows aligned films for glycine processed at 90 ˚C at a) 0.1 mm s-1 and b) 0.5 mm s-1. Films imaged at 20x, scale bar is 100 μm, and rotation of sample relative to shearing direction is indicated with arrow.

Figure 14. Film rotation shows aligned films for glycine processed at 90 ˚C at a) 0.1 mm s-1 and b) 0.5 mm s-1. Films imaged at 20x, scale bar is 100 μm, and rotation of sample relative to shearing direction is indicated with arrow.

Figure 15. GIXD images and peak shapes the different types of films that were obtained for (a) wide glycine crystals (b) needle like glycine crystals (c) thick crystalline deposits of acetaminophen and (d) spherulitic crystals of acetaminophen.

Figure 16. GIXD and corresponding integration patterns obtained for a), b) α glycine, c), d) β glycine Notice the difference in peak intensity as the samples are rotated for highly aligned glycine samples. Sample alignment biases the peak intensity, accounting for differences between experimental and simulated PXRD data.

Figure 17. GIXD and corresponding integration patterns obtained for a) acetaminophen Form I and b) acetaminophen Form II. Both forms crystallized with the (0 1 0) plane parallel to the substrate. GIXD peaks in Form I are dispersed due to the sample having more powdery character. Only perpendicular orientation is shown for

Figure 18. Representative scans obtained from integrating 2-D grazing incidence X-ray diffraction (GIXD) patterns. Dashed patterns are literature reported data a) α glycine formed at 70˚C, 0.03 mm s-1, b) β glycine formed at 80˚C and 0.11 mm s-1, c) acetaminophen form I formed at 100˚C, 0.03 mm s-1, d) acetaminophen form II formed at 100˚C and 0.5 mm s^{-1}

Figure 19: Processing diagrams for a) glycine and b) acetaminophen as a function of solution shearing speed and temperature. Polymorph selection is influenced by the solution shearing speed. Column graphs indicate the relative occurrence of each polymorph in the films. Summation of the bar graphs over 1 for any condition indicates film formation with multiple polymorphs in one sample.

Figure 20: Amorphous to crystalline transition in (a) acetaminophen. (b) Carbamazepine is also shown emphasize that solution shearing has utility in many different molecular systems, however the complete study was not carried out for carbamazepine.

Figure 21. Transformation diagram showing how blade speed relates to the timescale of nucleation and overall crystallization for acetaminophen thin films sheared at 90˚C.

Figure 22. General shape of a time temperature transformation diagram (TTT) with features (1, 2, 3) marking significant points for nucleation and growth. Fundamentally, the balance between nucleation and growth creates the characteristic curved shape.

Figure 23. Theoretical derivation of growth rate and labeled schematic of a growing crystal.

Figure 24: Example of growth rate calculation for a film processed at 80 degrees, 0.3 mm/s, showing a relatively stable growth rate calculated over the time period of 4 minutes.

Figure 25: a) An ideal case of crystallization, where ImageJ can accurately detect the crystal. b) an example of two crystals merging and skewing the measurement. c) Stick slip during the shearing process creates patterns in the crystal that makes the crystal discontinuous. d) Thin films have low intensity crystal formation that cannot be distinguished form the background

Figure 26. Schematic description of solution shearing being used to isolate polymorphs, as outlined in this study

List of Tables

Table 1: Observed polymorphism for glycine and acetaminophen with corresponding stabilities. Thick films contained the more stable polymorph.

Table 2: Growth rates for films formed at 80 ˚C and 90˚C. Shearing blade speeds ranged from 0.3 -1 mm s^{-1},.

Table 3: Example of growth rate calculation for a film processed at 80 degrees, 0.3 mm/s, showing a relatively stable growth rate calculated over the time period of 4 minutes.

*Calculations completed for a trial where A = 6210 µm^2 and P = 316 µm (R actual = 30.04 µm)

1. Abstract

In the pharmaceutical industry, significant resources are allocated to control the stability and solubility of a drug product, as the drug needs to be stable during processing and storage, and follow predictable dissolution kinetics in the body. Recently, enhancing solubility of poorly soluble drugs has become an area of study; many new candidate drug molecules are not pursued for further development because their low solubility makes them ineffective in the body.

The crystal morphology and the packing (polymorphism) of the pharmaceutical compound in the solid drug product determines the solubility and the associated bioavailability. For small organic molecules, most drug products are stored and ingested as solid forms. Controlling the crystallization process is necessary to isolating the selected solid form for development. If we are able to enhance the solubility of a drug through changing the crystal structure, then more candidate drugs can be pushed further in development.

We look to control the formation of amorphous and metastable crystalline solid-state phases to improve the solubility of the active pharmaceutical ingredient (API). Non-equilibrium (including metastable polymorphs and amorphous solid phases) formulations are a promising route for increased solubility since the non-equilibrium solid phase is, by definition, less stable than the equilibrium phase. The search for polymorphs with better solubility, coupled with federal guidelines to characterize all known polymorphs, have pushed pharmaceutical companies to carry out extensive searches in the API development phase to identify as many drug polymorphs as possible.

However, there are no generally applicable routes for finding polymorphs. Many different trial-and-error methods are combined and employed to induce polymorphism. Developing a robust system to screen for polymorphs and isolate metastable forms motivates this work towards solubility control in small organic pharmaceuticals.

Recently, a solution based crystallization technique termed solution shearing has been extensively utilized to control the polymorphism of organic semiconductors and tune device performance. Giri et al. have previously showed that in solution shearing, one-dimensional confinement is responsible for obtaining metastable polymorphs of organic semiconductors. Motivated by this previous work showing polymorph control, we apply the solution shearing technique to pharmaceutically relevant systems.

Previous studies have outlined numerous routes to stabilize various polymorphs of glycine and acetaminophen, making them ideal molecules to understand the influence of one-dimensional confinement on API polymorphism. In this work, two model pharmaceutical compounds, glycine and acetaminophen, were crystallized using a flow coating technique termed solution shearing to create thin films with controllable polymorphism. Thin films were characterized using cross-polarized optical microscopy and grazing incidence X-ray diffraction. Films crystallized as different polymorphs (α and β for glycine and form I and form II for acetaminophen) by controlling processing temperature and shearing speed. The amorphous phase of acetaminophen was also stabilized, and the kinetic transformation to the metastable form II was studied. We show that one dimensional confinement plays a significant role to stabilize metastable polymorphs and amorphous phases. We foresee that solution shearing will have vast utility in high throughput screening of candidate drug molecules to determine the polymorphic landscape with minimal material usage.

2. Introduction and Background

2.1 Pharmaceutical development

The pharmaceutical industry is a multibillion industry that produces essential drug products.[1] Drug development is regulated throughout each stage to ensure standardized and controlled products are provided to the consumer. In the drug development process, a single Food and Drug Administration (FDA) approved drug begins with 5,000-10,000 candidate molecules that are narrowed down to a few hundred for further pre-clinical studies (figure 1).[2] Many of these drugs are eliminated from drug candidacy due to poor aqueous solubility, rendering them ineffective in the body.[3] Others can be eliminated due to an inability to control the crystallization process to produce a desired drug form.[4] These drugs are inefficient to pursue for further development.
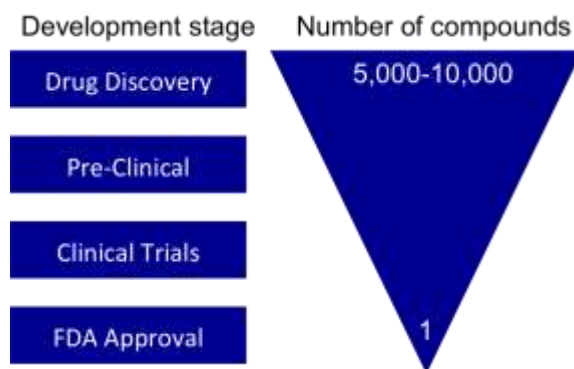
Figure 1. Development of a single FDA approved drug begins with several thousand candidate molecules.

In the drug discovery phase, the efficacy of the drug is assessed and candidate drugs are characterized, consistent with FDA requirements. Relevant to this work, the FDA mandates that (1) polymorphs (crystal forms), solvates, hydrates and amorphous forms of drug compounds are known, (2) potential phase transformations are well characterized and (3) each polymorph is patented separately for development.[5] This is to ensure that the drug form selected for development is optimized for balance between stability and solubility.

2.2 Stability, solubility, and bioavailability

Important considerations for pharmaceutical development include the stability, solubility, and bioavailability of the drug in the body.[6] Many of the newer drug candidates present the challenge of low aqueous solubility, rendering them less effective in the body and unable to elicit the desired drug response.[3] Further, once dissolved, the drug must become bioavailable, or present in circulation for drug

delivery. Improving low solubility and enhancing dissolution kinetics in drug materials is an ongoing field of study.[7] The drug solid state has an important impact on the solubility profiles.

Shown in figure 2a, two crystalline forms have different solubility behaviors, and to maximize the bioavailability, the form with higher solubility could be selected for development at the cost of decreased stability.[8] Figure 2b shows an additional advantage of selecting a metastable form, where the amorphous state is released more rapidly compared to crystal forms.[9]
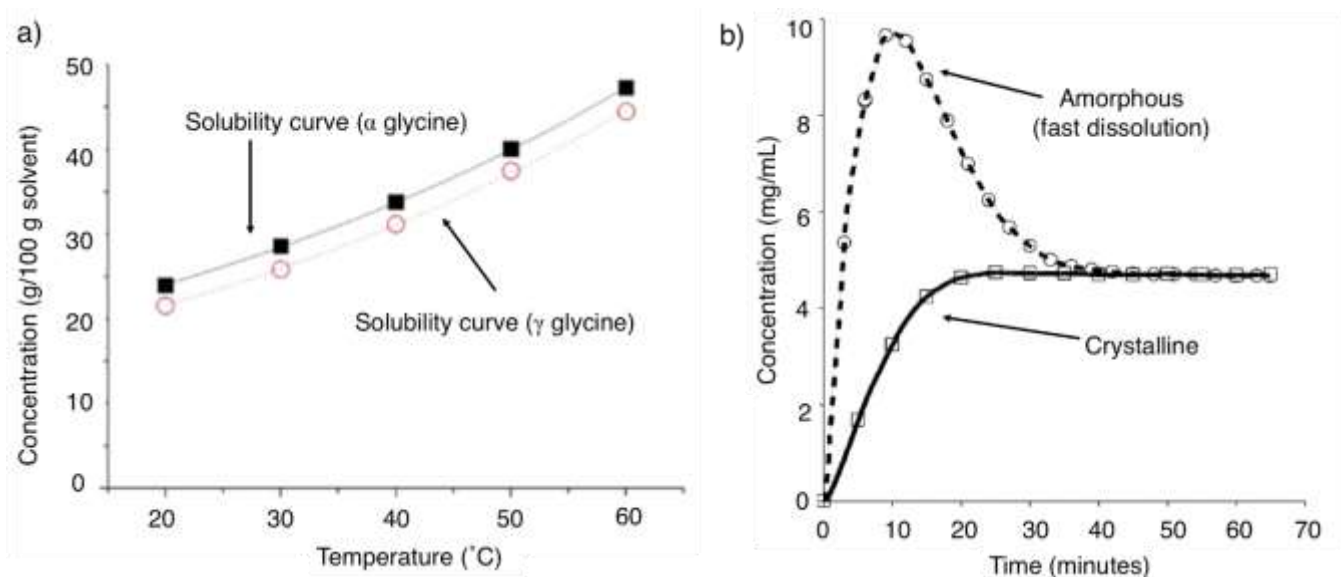

Figure 2. a) Two crystal forms of the same material have different solubilities. Reprinted with permission from Kim, J.-W.; *Cryst. Growth. Des.* **2012,** *12* (10), 4739-4744. Copyright 2017. American Chemical Society. b) Amorphous and metastable crystal forms display enhanced dissolution kinetics. Adapted from Brittain, H., *Am Pharmaceut Rev* **2014,** *17* (3), 10-6.

If candidate drugs have improved solubility and bioavailability, these candidates can be screened with greater emphasis on their biological efficacy. Numerous methods are being researched or used in industry to increase the biological activity of insoluble drugs, but at the cost of increased complexity during formulation.[7] We aim to control the formation of amorphous and metastable crystalline solid-state phases to improve the solubility of the active pharmaceutical ingredient (API).[10] Non-equilibrium (including metastable polymorphs and amorphous solid phases) formulations are a promising route for increased solubility since the non-equilibrium solid phase is, by definition, less stable than the equilibrium phase.

2.3 Solid phases and polymorphism

Solid phases of a given compound can take on many different forms including amorphous solids and several crystalline forms (polymorphs).[10] Polymorphism describes the different molecular packing that composes the crystalline forms of a material. The same compound can assemble in different unit cells through bond rotations and intermolecular forces that influence molecular packing (figure 3). Amorphous materials have no long-range order associated with the arrangement of the molecules.
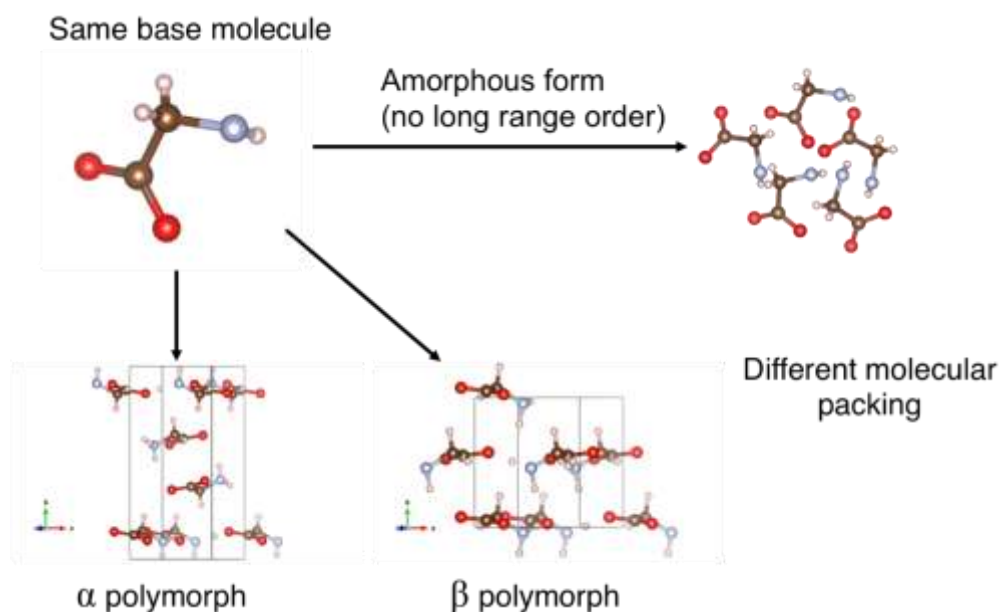
Figure 3. Different solid states form through assembly of the same molecule in different ways. Amorphous materials have no long-range order associated with molecular arrangement. Polymorphs have ordered unit cells with dissimilar molecular packing that creates different unit cell shapes and sizes.

The energetically activated nucleation and growth processes govern formation of different crystalline phases and different environments (temperature, concentration, pressures, etc.) can provide the energy required to isolate a specific crystal form.[11-12] Different polymorphs have different relative stabilities (figure 4), which lead to unique physical and chemical properties, most important to pharmaceuticals being the solubility and bioavailability, as previously discussed.
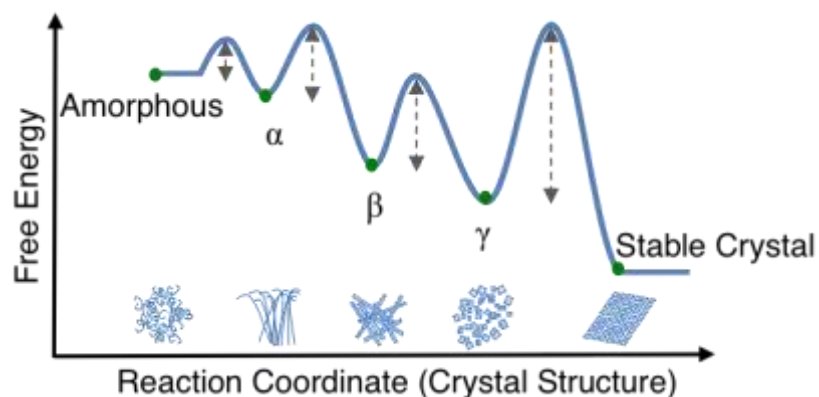
Figure 4. Crystallization is an energetic event with intermediate crystal forms existing. Prior to arriving at the most thermodynamically stable crystal, a drug may pass through metastable crystal forms.

The search for polymorphs with optimal chemical properties, coupled with federal guidelines to characterize all known polymorphs, have pushed pharmaceutical companies to carry out extensive searches in the API development phase to identify as many drug polymorphs as possible. However, there are no generally applicable routes for finding polymorphs. Many different trial-and-error methods are combined and employed to induce polymorphism, including variable solvent input, thermal cycling, and additives (including co-crystals, co-solvents and excipients).[13] Other methods to obtain polymorphs are being researched, such as computational structure prediction, vapor exposure, crystallization on treated surfaces and capillary crystallization.[14-17]

Recently, nanoscale confinement methods such as crystallization in controlled pore glass and nano-drops have shown great utility in obtaining metastable polymorphs of numerous pharmaceutical compounds.[18-22] These results suggest that there is a fundamental connection between confined environments and metastable crystallization. However, these methods do not yield significant amounts of the metastable polymorph for further testing and processing.

2.4 Crystallization processes

In industry, batch and semi-batch processes are more universally used compared to continuous processes. To achieve the desired crystal size distribution, shape and polymorph, careful process control is necessary.[23] Controlling a crystallization process relies on regulation of the process's operation relative

15

to conditions that result in supersaturation, and therefore nucleation or growth. Primary components that are controlled include the temperature, concentration and use of solvents or other additives that can push equilibrium conditions towards or away from crystallization conditions (figure 5). Selection of the appropriate method of controlling supersaturation is a primary concern operating in the desired nucleation and growth regimes (figure 5). Temperature has been shown to be a fundamental parameter in directing polymorph formation both in bulk and thin films, as it directly influences the supersaturation.[24-25] Control of solute concentration is another parameter that is traditionally important to industrial crystallization; phase stability can be
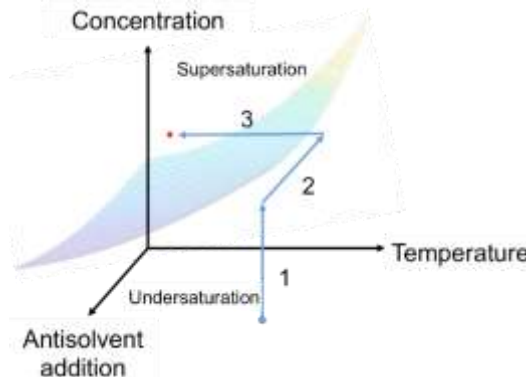

Figure 5. Traditionally, the parameters of temperature, concentration and solvent selection are extensively used to influence the supersaturation of a system. Through this the nucleation and growth regimes are selected for desired crystallization behavior.

linked to crystallization from specific solute concentrations.[26] Since nucleation requires aggregation of precursors to achieve a critical effective size, using a low concentration can limit interactions and increase induction time required for nucleation (and decrease the number of nucleation events due to decreased supersaturation), allowing a growth dominant regime to occur.[27] The converse is also true, where high concentration will result in large supersaturations, allowing uncontrolled nucleation. Controlling the number of particles (by controlling nucleation) and size of particles (by controlling growth) can thus be achieved by controlling the concentration profile.

Solvent selection (including antisolvents) play a significant role in dictating the final crystallization product by influencing the crystal polymorph, crystal shape and generally, the kinetics of crystallization.[28] This is because solvents can influence the width of the metastable region, where polymorph selection occurs. This makes new polymorphs accessible when they would not be with a different choice in solvent.[29] Additionally, solvents can assist the formation of solvates through modulating the aggregation of crystal precursors with solvent inclusion in crystal forms.[28] Further, the

strength of the solvent-solute interaction can lead to control over the growth rate, and therefore size of the final crystal product.

2.5 Polymorphism obtained using solution shearing

In the field of organic electronics, control of polymorphism is also of great importance for reliably and consistently preparing high performance devices. A solution based crystallization technique termed solution shearing has recently been extensively utilized to control the polymorphism of organic semiconductors.[25, 30] Solution shearing can be scaled up for high-throughput industrial production while preserving laboratory scale results.[31] Giri et al. have previously showed that in solution shearing, one-dimensional confinement is responsible for obtaining metastable polymorphs of organic semiconductors.[32] In an organic semiconductor, changing the shearing speed influences crystallization to produce different unit cell shapes and sizes (figure 6a). This allows for tunable charge carrier mobility to optimize device performance (figure 6b)
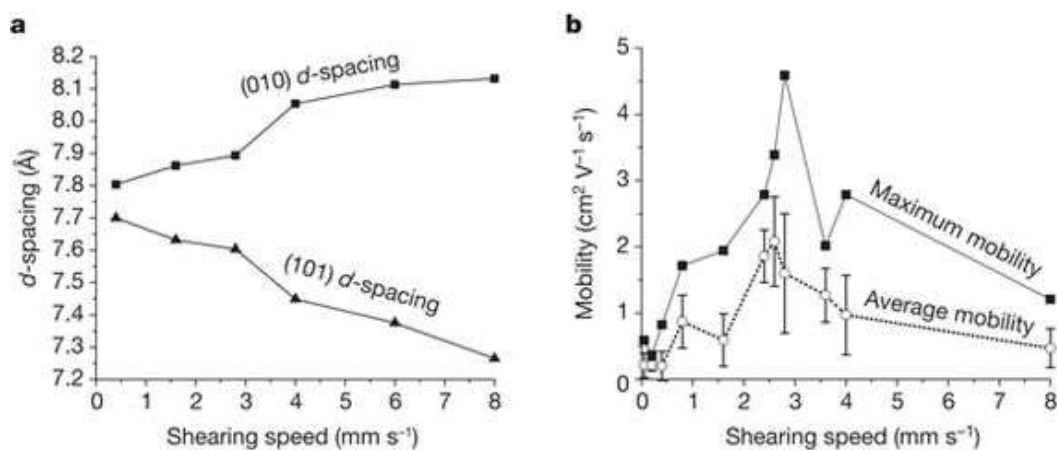
Figure 6. In solution shearing, changing the blade speed optimizes device performance through a) changing the shape and size of the unit cell (d-spacing) and b) increasing charge transport as a result of polymorphism. Figure used with permission from Giri, G. *Nature* **2011,** *480* (7378), 504-508.

With the use of solution shearing, we build on traditional crystallization techniques (temperature, solvent, concentration control) and incorporate the parameters of confinement and evaporation rate. The integration of these parameters allows us to access different crystallization regimes that report the existence of new polymorphs.[32] The evaporation rate has reportedly allowed for selection of polymorphic

forms with controllable change in the crystal shape and size.[33] Confinement has been shown to be a parameter that influences polymorphism and crystallization, however confinement is a surface dominated phenomenon that cannot be effectively accomplished in a bulk crystallization system.[19] If we wish to utilize the fundamental information that polymorphism arises from confinement, then we must use a surface dominant (as opposed to volumetric) approach to crystallization. Shearing is a confined system, as the thickness of thin films is dimensionally limited by surface tension and the spacing between the shear surface and the blade.

2.6 Model pharmaceutically relevant molecules

Glycine (figure 7a), the simplest amino acid, is often used in drug formulations as an excipient to enhance crystallization. Three polymorphs crystallize commonly at normal pressures and temperatures. They have the following relative stabilities $\gamma > \alpha > \beta$.[19] The α form is most abundant, with bulk β transforming to α in ambient conditions.[19]
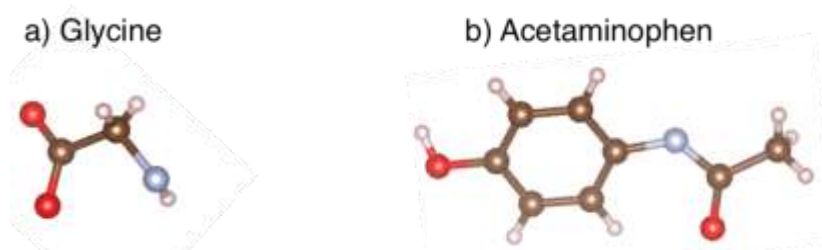
Figure 7. Molecular structure a) glycine and b) acetaminophen used in this study

Acetaminophen (figure 7b) is a fever and pain reducer. Crystalline tablet forms are commonly used, as well as liquid-gel capsules that have rapid release kinetics.[34] The common polymorphs are Form I (most stable) > Form II > Form III (least stable).[35]

2.7 Outlook

Previous studies have outlined numerous routes to stabilize various polymorphs of glycine and acetaminophen, making them ideal molecules to study.[35-36] Here, we look to understand the influence of one-dimensional confinement on API polymorphism. We show controllable polymorphism in glycine and acetaminophen through applying the solution shearing method to these molecules. The morphology and texture of the thin films was characterized using optical microscopy and grazing incidence X-ray diffraction. We also stabilize the amorphous form of acetaminophen and study the transformation to

18

crystalline phases. The growth rate of crystals was studied throughout the phase transition in attempts to gain insight to the mechanisms of nucleation and growth. We foresee that solution shearing will have vast utility in screening candidate drug molecules to determine the polymorphic landscape with minimal material usage.

3. Materials and Methods

3.1 Materials

Glycine (98.5%) and acetaminophen (98%) were obtained from Sigma-Aldrich. Protocol® deionized water (100% v/v) was obtained from Thermo Scientific. Small organic molecules were dissolved in deionized water at a concentration of 10 mg/mL for all experiments.

Shearing set up preparation (assembly, blade and substrate)

Films were formed using a solution shearing setup consisting of a heat source (IKA RTC Basic hotplate), linear driver (Harvard Apparatus PHD 2000 infuse/withdraw syringe pump), substrate, and shearing blade. The volumetric flow rate and input diameter on the syringe pump were set such that a desired linear shear speed was obtained.

Silicon wafers cut into approximately 1 cm^2 pieces were used as substrates. Wafers from Silicon Quest International or University Wafer were 100 mm in diameter and 500 µm thick with native oxide surface and crystallographic orientation <1 0 0>. Silicon wafers were washed using toluene, acetone, deionized water, and isopropyl alcohol then dried using air. Prior to shearing, clean wafers were exposed to ultraviolet light (BioForce UV/Ozone ProCleaner) for at least 15 minutes to render the surface hydrophilic.

A silicon wafer shearing blade was functionalized with 1H,1H,2H,2H-Perfluorooctyltriethoxysilane (FTS) (98%, Sigma-Aldrich). To functionalize the surface, a wafer was cut to size and cleaned with toluene, acetone, isopropyl alcohol and dried with air. The clean blade was then placed in a UV/ozone chamber for 15 minutes. The UV activated blade was sealed in a vacuum desiccator with 200 uL of silane and left under vacuum for 8 hours to form a vapor deposited hydrophobic surface.

Solution shearing technique

Clean wafer substrates were removed from the UV chamber prior to shearing. After securing the wafer to the hotplate with double sided tape (3M). The FTS functionalized shearing blade was placed on top of the substrate and ~20 µL of prepared solution (10 mg/mL) was placed at the blade/substrate interface.

Capillary action distributed the solution between the blade and substrate. Translation of the blade across the substrate created the evaporation front, and evaporation of the solvent gave rise to the solid thin film. The range of temperatures (70-100 ˚C) and shearing speeds (0.027 – 3 mm s^{-1}) were selected to obtain uniform thin film behavior. The films were characterized using white light interferometry, polarized optical microscopy, and X-ray diffraction.

3.2 Characterization

Interferometry

A Zygo NewView 7300 Optical Surface Profiler/white light interferometer was used to measure film thickness. Films were scratched to reveal the silicon substrate. Samples were sputter coated and the relative difference between peak (film surface) and valley (scratched region with exposed substrate) was taken as the film thickness. Measurements were taken in several regions and line scans were taken to obtain roughness and thickness variation across the sample. MetroPro software was used to collect and analyze data.

Microscopy

Optical images were acquired on a Zeiss Axio A.1 Microscope with 5x, 10x, 20x, 50x objective lenses, using brightfield and cross-polarized light. Polarized samples were imaged in several orientations relative to the direction of shearing to show regions of alignment (figure 8).

Figure 8. Using cross-polarized optical microscopy, crystal alignment can be studied. Similarly aligned domains have similar intensities as samples are rotated.

For time dependent studies, optical images were captured at discrete timepoints to determine growth rates.

Image analysis

Time series optical images were further analyzed using ImageJ. All images collected from one film were opened in the software for batch processing. Using the scalebar embedded in the images, the scale was set and globally applied to all images. The images were reduced to 8-bit and then threshold adjusted

21

such that crystalline regions were distinct from the amorphous background. Finally, the images were made binary (black and white). Parameters were set for collection; primarily the area and perimeter were desired. The analyze particles function was run, analyzing the crystal as the particle in this application. The output area and perimeter were further reduced to growth rate data in excel.

Grazing incidence X-ray diffraction (GIXD)

X-ray diffraction was used to determine the structure of materials through interaction of the incident x-rays with electrons to produce a diffraction pattern. Compared to metallic and inorganic materials, the organic materials that are studied herein have fewer electrons to participate in the diffraction phenomenon contributing to low diffraction strength.[37] Using a synchrotron source of X-rays was necessary, due to the high flux and X-ray energy required to produce a reasonable signal.

Further, thin films have inherently lower signal due to the small amount of material on each sample. To produce appreciable signal, grazing incidence X-ray diffraction (GIXD) is used to amplify signal intensity. To accomplish this, the incident angle of the X-ray beam must be carefully selected and tuned such that total internal reflection within the film occurs.[37] Too high of an angle will lead to penetration of the substrate while too low of a sample will reflect off the film without sampling a large area.

GIXD was carried out at the Cornell High Energy Synchrotron Source (CHESS). The D1 beamline incident X-rays ranged in wavelength 0.1162-0.117 nm throughout several runs. The incident angle was 0.15˚. Diffraction patterns were recorded using a Pilatus 200K detector located 160-180 mm from the sample. The 2D data was analyzed using the indexGIXS software package developed by Detlef Smilgies.[38] Fit2d was used to integrate 2D diffraction images to the 1D analog along constant radius from the beam center.[39] Mercury was used to produce simulated powder patterns from deposited crystallographic information (cif) files in the Cambridge structure database from previous studies.[40-43]

Through analyzing the location and shape of the Bragg diffraction peaks, both the polymorphic identity and film texture can be extracted. Film texture can also be summarized through observing characteristic GIXD patterns as they relate to the crystal packing. Figure 9b summarizes the relationship between film alignment and texture on the resulting GIXD patterns observed.
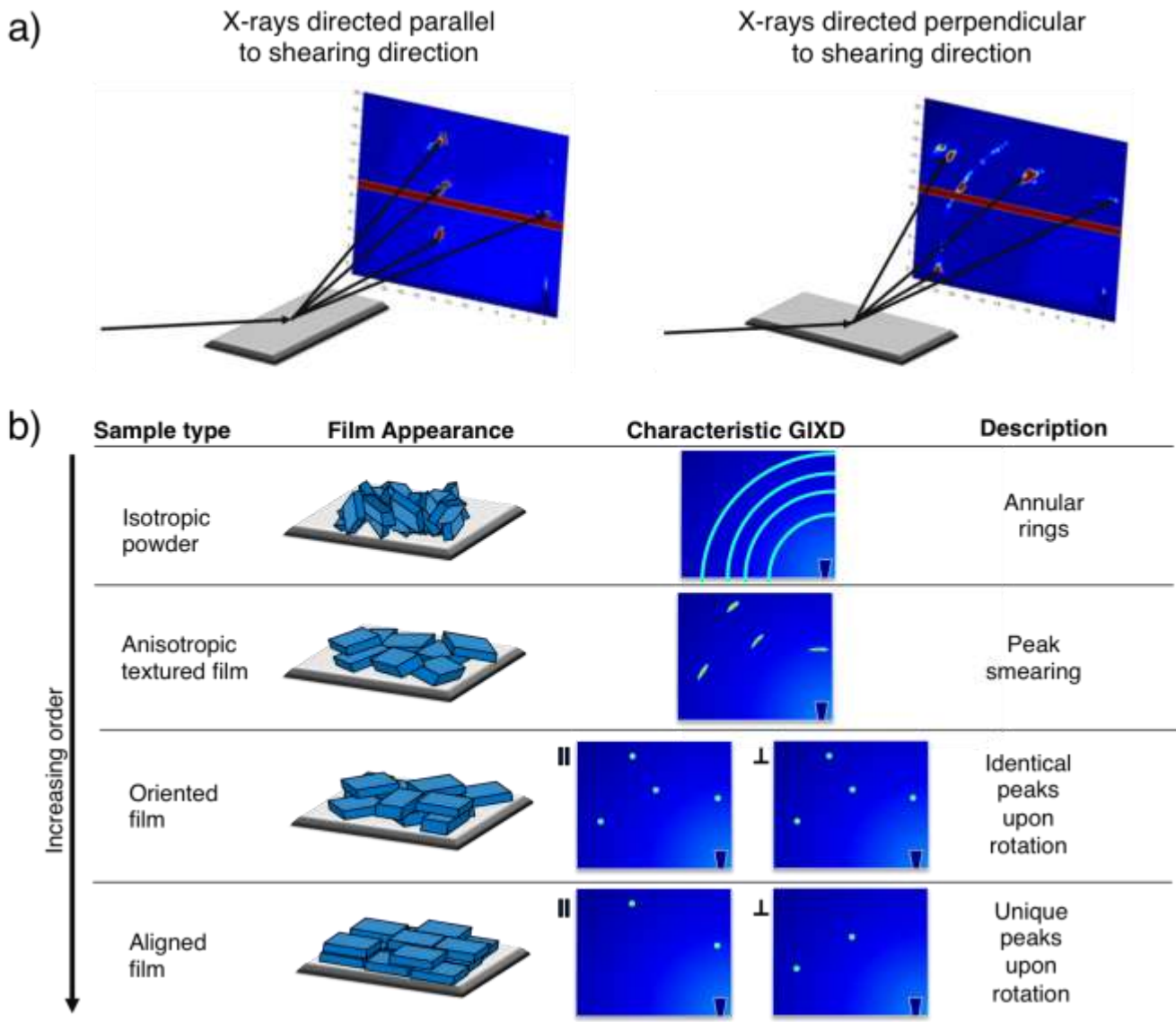
Figure 9: a) Schematic of diffraction measurements taken parallel and perpendicular to the blade direction. b) Characteristic film morphologies and corresponding GIXD patterns relevant to this work.

Beginning with the lowest degree of order, a powder diffraction pattern has crystallites in all orientations. The result is an annular ring, with the ring being composed of many diffraction peaks from each plane. As crystallites begin to orient on the substrate the rings begin to into peaks. However, misorientation of the sample on the substrate contributes to the peak broadening or smearing. As a film gains further order in an oriented sample, the same crystallographic face is always in contact with the substrate, with crystals having order in one dimension. In this case, rotating the sample does not introduce

any new crystallographic planes to the path of X-rays, resulting in identical peaks in any sampled direction. In an aligned film, there is further order of the crystallites, which assemble with orientation in the plane of the substrate and in the direction of shearing. Therefore, rotating the sample will introduce new planes to the path of the X-rays, resulting in unique Bragg peaks that correspond to each sampled direction (figure 9a).

4. Controlling Pharmaceutical Thin Film Crystallization using Solution Shearing

4.1 Film Thickness

Solution shearing was used to create pharmaceutical thin films of glycine and acetaminophen. In this method, a solution containing the solute of interest is placed between a bottom heated substrate and a top shearing blade. As the top blade is translated, solution is spread across the substrate and an evaporation front is created at the meniscus. As the solvent evaporates, the solution becomes supersaturated and the solute nucleates, and forms a solid thin film (Figure 10a).
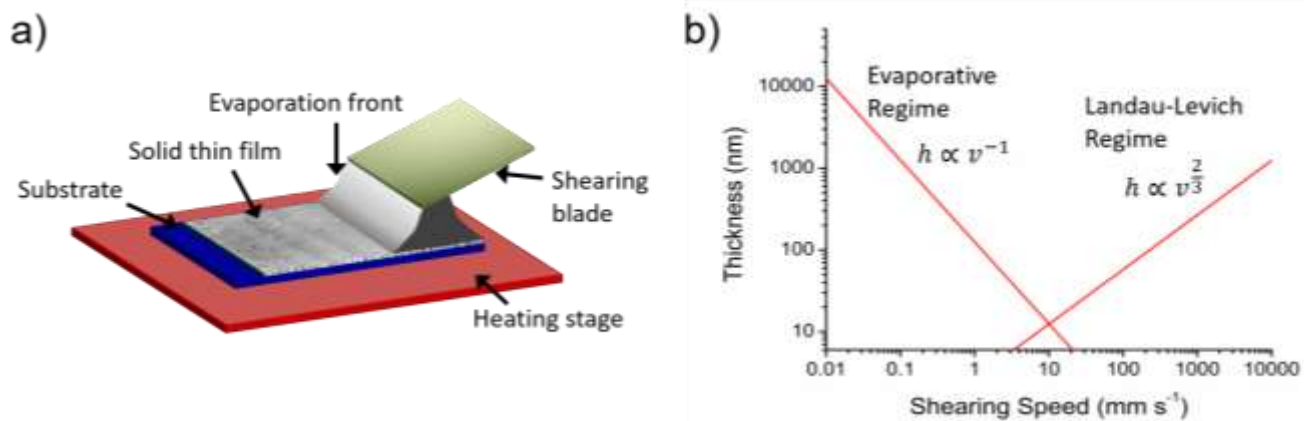

Figure 10. (a) Conceptual image of the solution shearing technique for thin film formation. (b) Evaporative and Landau-Levich shearing regimes. In the evaporative regime, film thickness decreases as shearing speed increases ($h \propto v^{-1}$). In the Landau-Levich regime, film thickness increases with shearing speed, ($h \propto v^{2/3}$). Trendlines adapted from equations outlined by Le Berre et al. with parameters updated to reflect the water-pharmaceutical system in this study.

According to theoretical work by Le Berre et al., the blade speed is a primary factor in controlling film thickness and the deposition regime, which can be either the evaporative regime or the landau levich regime.[44] In the evaporative regime, the timescales of the blade movement and solvent evaporation are similar. In this regime, crystallization occurs as the blade is moving across the substrate. In the Landau-Levich regime, the evaporation rate is slower than the timescale of the blade movement, and evaporation continues to occur after the blade has passed across the substrate. In this case, the solution flow caused by the blade has no effect in creating an ordered film and crystallization is dominated by just the evaporation.
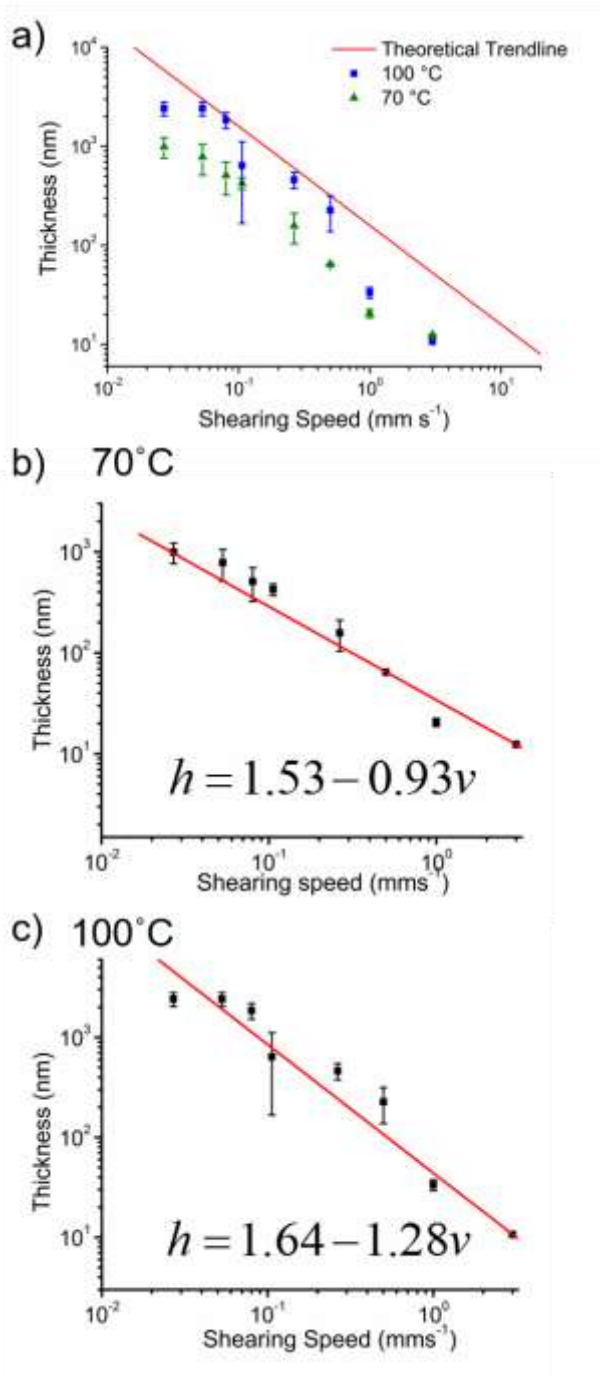
The theoretical relationship between shearing speed and film thickness is given by equation 1 in the evaporative regime.[44]

$$h = \frac{C}{\rho}\frac{Q_{evap}}{L}v^{-1} \tag{1}$$

This is shown conceptually in Figure 10b.

Here, the relationship between h (film thickness) and v (blade speed) is dependent on several system parameters. C represents the solution starting concentration, ρ the film density, Q_{evap} is the evaporation rate from the meniscus, L is the width of the film. Fluid dynamics define system characteristics with the blade speed being the variable in this study that dictates regime.

In the evaporative regime, the film thickness decreases as shearing speed increases (equation 1). Through collecting film thickness measurements from a set of glycine thin films, and linearizing data on log-log plot, the exponential dependence of film thickness on blade speed was determined. This provides insight on whether film deposition was occurring in the evaporative or the Landau-Levich regime. In the conditions explored in this work (70-100 ˚C, 0.01-3 mm s^{-1}), the films were formed under evaporative

Figure 11. (a) Film thickness data overlaid on theoretical evaporative regime trendline. Thickness measurements of glycine at (b) 70 ˚C with exponential factor of -0.93 and (c) 100 ˚C with exponential factor of -1.28. Exponential factors, suggest operation in the evaporative regime.

conditions (Figure 11). Consistent with the evaporative regime, the first order coefficient for film thickness and blade speed is negative, which indicates that the film thickness increases with decreasing

26

shearing speed. The exponential factors for the relationship between the blade speed and thickness, processed at 70 ˚C and 100 ˚C, were -0.93 and -1.28 respectively. This is different than the ideal exponent of -1, showing some deviation from ideality, but still consistent with trends in the evaporative regime.

In the evaporative regime, the timescales of blade speed (which controls fluid deposition) and evaporation (which controls solid state formation) are similar. Therefore, controlling either the blade speed or the substrate temperature impacts the resulting solid-state thin film thickness and morphology.

4.2 Film Morphology using Optical Microscopy

Optical microscopy was used to observe morphology of the thin films. Representative samples that were solution sheared at 90˚C, using various blade speeds, show the effect of shearing speed on the crystalline morphologies of glycine and acetaminophen (Figure 12). For glycine, crystalline films were formed in all cases. Large, continuous crystalline domains were obtained when the film was cast at speeds of 0.1 mm s^{-1} or slower. Thinner, needle-like crystals appeared at faster speeds. In both cases, the crystals were aligned with the shearing direction (Figure 13). Acetaminophen films had a different morphology with changing shearing speed as well. At slow solution shearing speeds (0.1 mm s^{-1} and slower, crystalline films were deposited. The film texture was non-uniform, with stick-slip motion during shearing causing
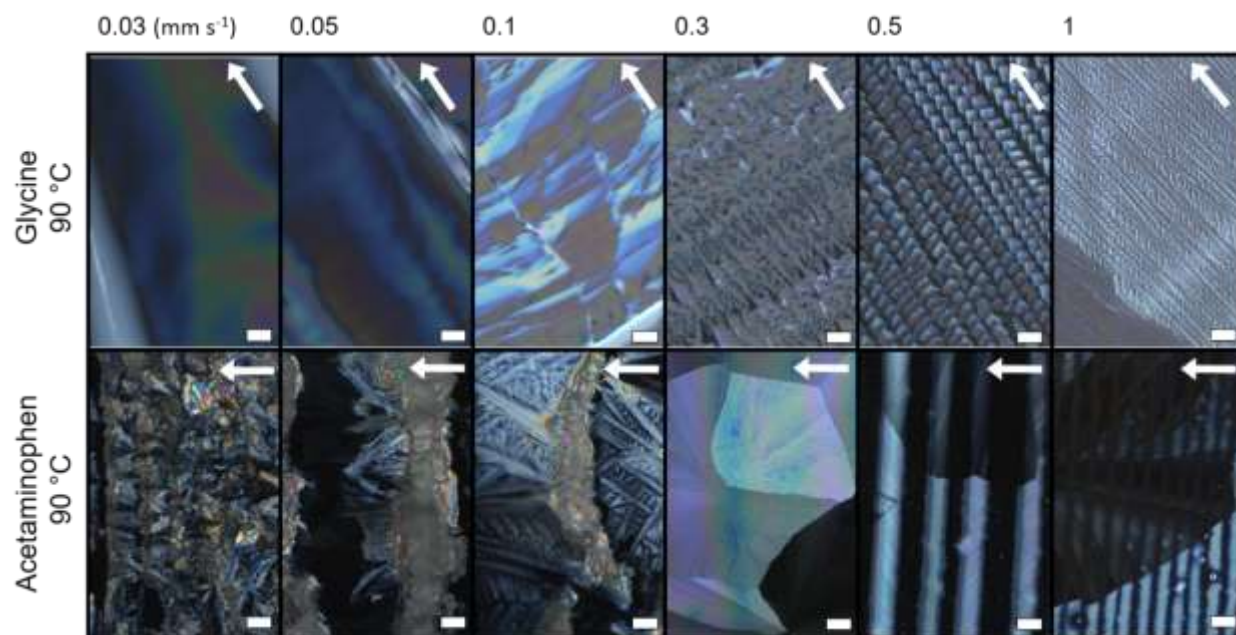

Figure 12. Glycine and acetaminophen thin films formed at a range of blade speeds, at. Films imaged at 20x, scale bar is 20 μm, and sample orientation relative to shearing direction is indicated with arrow.

27

bands of thick and thin crystalline regions.[45] Shearing speeds of 0.3 mm s^{-1} or greater (Figure 14) produced an amorphous thin film that transformed into a spherulitic crystalline film. These crystalline films appeared to be isotropic in the plane of the substrate.

The alignment of crystals was studied under polarized light, where sample rotation will cause similarly aligned domains to appear bright or dark as a result of twinning. Figure 13 shows sample rotation for glycine, the case where aligned domains are present. As the sample is rotated (indicated by the arrow), the crystallites phase through dark and bright intensities.
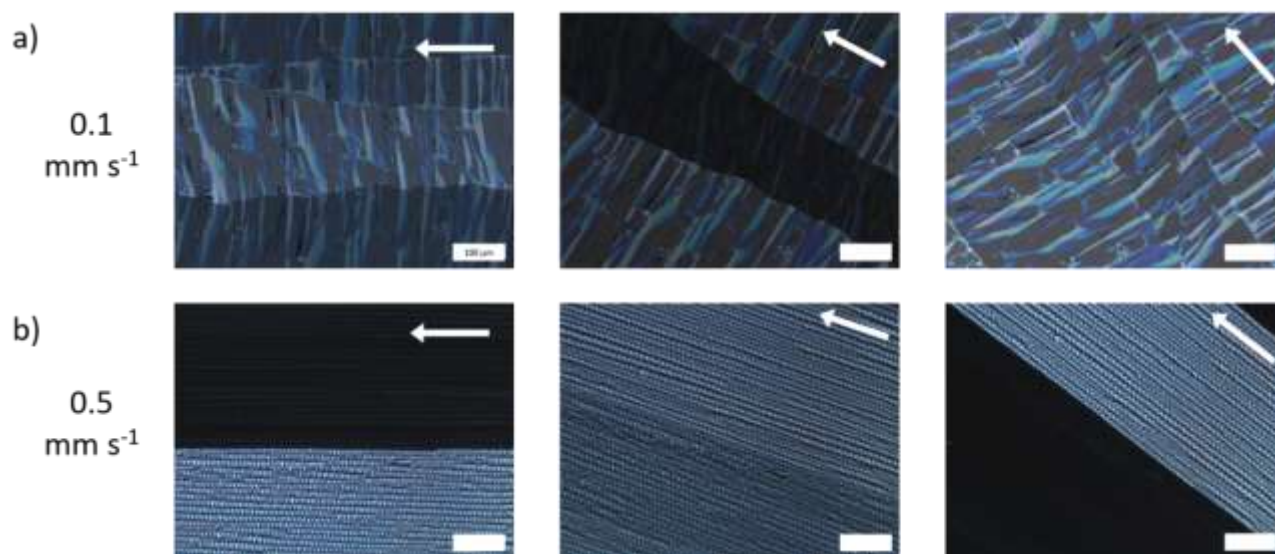

Figure 13. Film rotation shows aligned films for glycine processed at 90 ˚C at a) 0.1 mm s-1 and b) 0.5 mm s-1. Films imaged at 20x, scale bar is 100 μm, and rotation of sample relative to shearing direction is indicated with arrow.

Polarized light analysis for acetaminophen yielded additional information. Using sample rotation, the alignment of crystallites was studied. For the films formed at slow speeds (Figure 14a) there does not appear to be any large-scale change in the light characteristics with sample rotation, indicating that crystals are not aligned. However, a different type of solid state phase change is seen at faster blade speeds. In figure 14b, directly after solution shearing, the film was amorphous. Polarized light microscopy is able to distinguish amorphous and crystalline samples, because amorphous materials are not birefringent under polarized light. For acetaminophen, either amorphous or crystalline phases could be obtained after

28

solution shearing, with the amorphous phase eventually transforming to a crystalline film over a longer time scale.
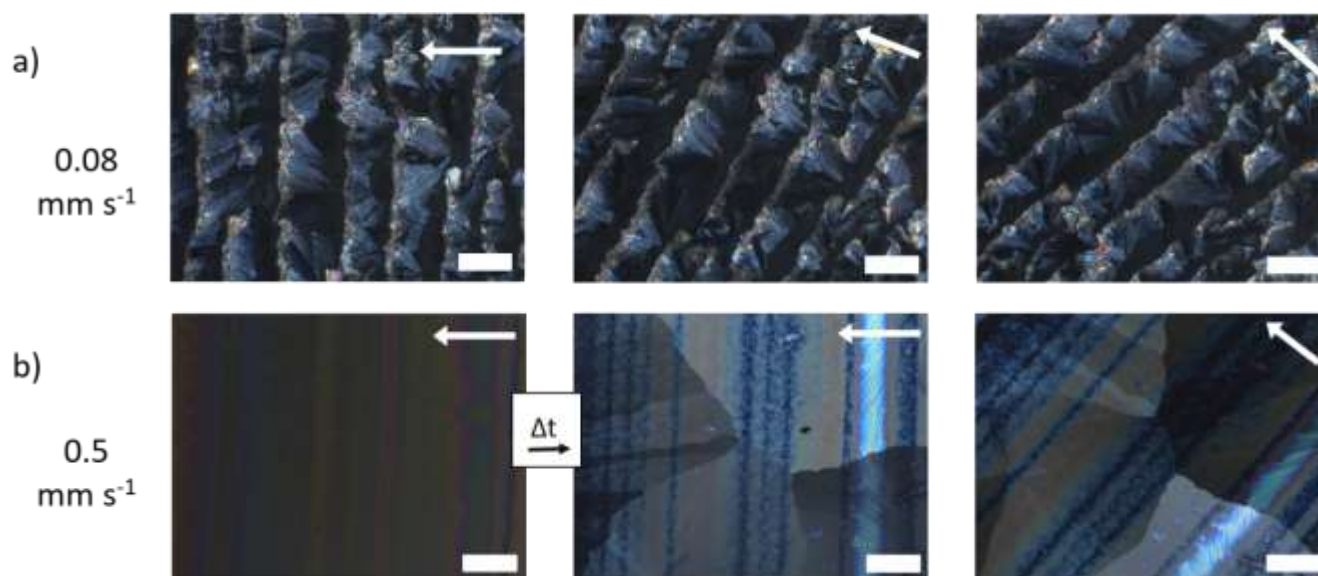

Figure 14. Film rotation shows aligned films for glycine processed at 90 ˚C at a) 0.1 mm s-1 and b) 0.5 mm s-1. Films imaged at 20x, scale bar is 100 μm, and rotation of sample relative to shearing direction is indicated with arrow.

When the films crystallized from the amorphous phase (at faster speeds, figure 14b) there was a central nucleation point with spherulitic growth outwards from the nucleation point. Therefore, there was no alignment of crystals with the shearing direction.

4.3 Film Texture using GIXD

This optical information is corroborated by GIXD (figure 15). For glycine sheared at fast and slow blade speeds, the Bragg peaks appear as distinct peaks with minimal spreading (figure 15a, b). This tells that the samples are oriented with respect to the substrate. Further, we observe different peaks when sampling with the X-ray beam directed parallel and perpendicular to the blade direction during solution shearing (not pictured). This indicates that, in addition to the sample being oriented, it is aligned (aligned with respect to two axes). Finally, the two samples have unique peak locations, indicative of polymorphism, which will be discussed later.

The GIXD analysis for acetaminophen is consistent with optical information, where sample rotation does not produce any Bragg peaks. The films formed at slow shearing speeds have broad peaks (figure 15c). This indicates that the film has most crystallites with the same orientation with respect to the

substrate, but that there is some misorientation, creating texture in the sample. The film is anisotropic and

textured. The films formed at faster speeds (figure 15d) have less spread in the peaks, showing better
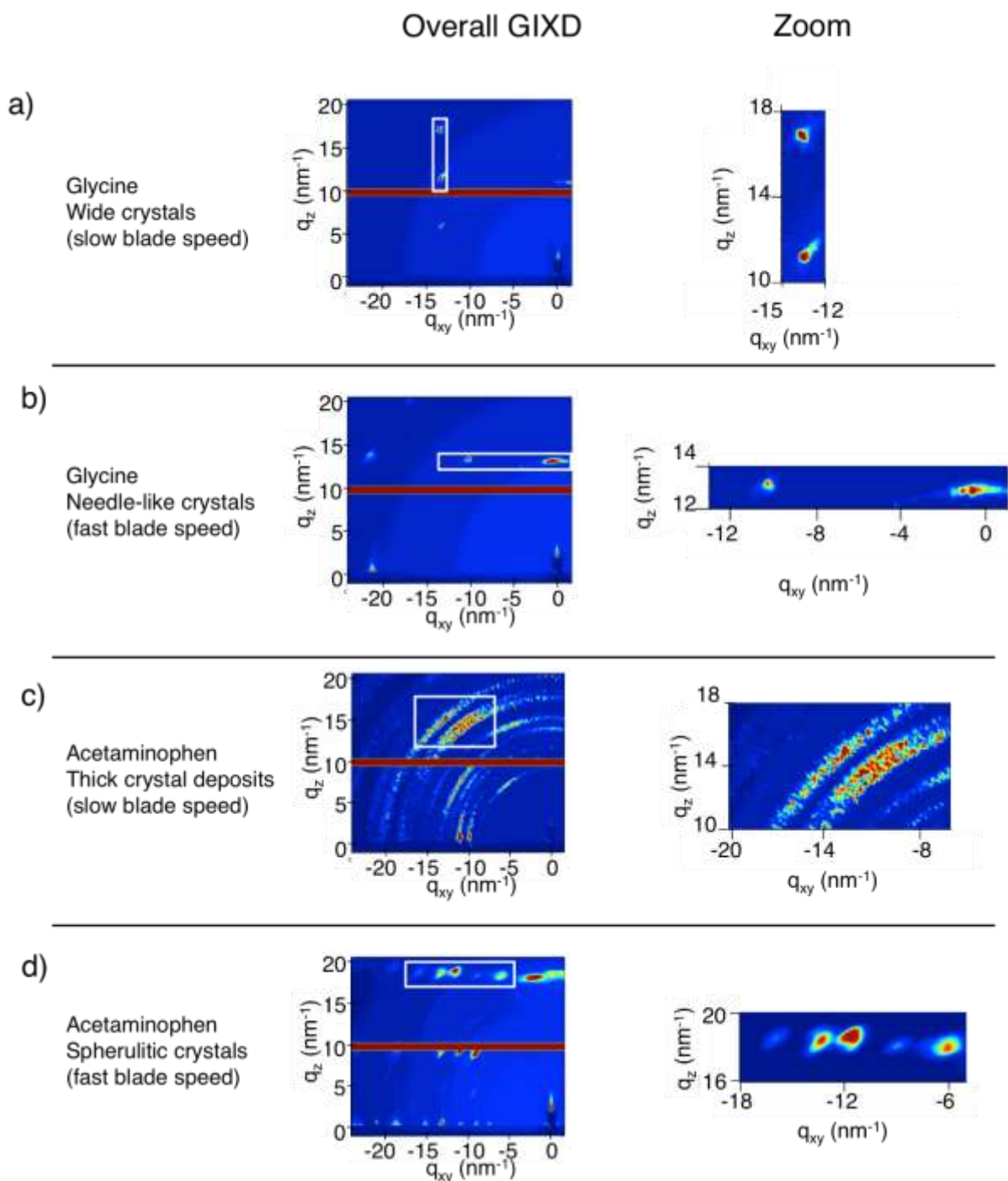
Figure 15. GIXD images and peak shapes the different types of films that were obtained for (a) wide glycine crystals (b) needle like glycine crystals (c) thick crystalline deposits of acetaminophen and (d) spherulitic crystals of acetaminophen.

registry with the substrate. However, upon sample rotation, the same peaks appear in the parallel and

perpendicular directions. These films are oriented but not aligned. Again, the peak locations are different

30

for these two samples, which suggests that acetaminophen polymorphs were obtained which will be discussed more as it pertains to polymorphism.

Solution shearing provides an avenue in this work to form thin films ranging from nanometers to microns in thickness. From the optical images, it appears that the solution shearing has some influence over alignment in glycine crystal growth. At fast shearing speeds, many needle-like crystals are formed, each originating from a nucleation point, due to high supersaturation. The supersaturation remains high, causing nucleation to occur throughout the shearing process. At the slower shearing speeds, there appear to be fewer nucleation points, as crystals are wide and aligned connected domains. This is because supersaturation is lower compared to faster shearing speeds, allowing growth to occur instead of nucleation. In glycine, the growth direction extends along the blade direction. The coupling of nucleation and coating timescales for glycine film formation indicates that the process had an impact on molecular assembly, through inducing a concentration and temperature gradient and allowing crystal growth along the direction of coating. Shearing has the ability to control operation in the metastable region near supersaturation to dictate balance between nucleation and growth. Balancing the blade speed and temperature of the substrate thus controls film morphology.

For acetaminophen, some conditions produce films that are initially amorphous, and there is some patterning of the film with features perpendicular to the blade direction caused by stick slip motion, as noted by the banding that appears. The banding is seen in both slow and fast shearing conditions. At slow shearing speeds, the crystalline deposits are the result of many nucleation events occurring, as the time scale for induction of nucleation matches the time scale of solution shearing speed and that of the evaporation rate. On the other hand, at the faster coating speeds, the time scale of induction of nucleation is slower than that of the solid film formation, so the film solidifies as an amorphous phase. With the conditions studied, solution shearing was not able to access a processing condition where limited nucleation was followed by growth for acetaminophen, like that seen for glycine.

5. Controlling Polymorphism using Solution Shearing

Grazing incidence X-ray diffraction (GIXD) was used to determine the crystal polymorph of glycine and acetaminophen. GIXD is a specialized technique that is used to obtain crystal structure information, specifically for thin films. Previously, the film texture using GIXD was discussed. In that analysis, it was noted that samples solution sheared under different conditions produced different Bragg peaks, consistent with polymorphism.

Here, peak indexing (using indexGIXS) was used to determine the polymorphic phases present by matching simulated GIXD patterns (from input unit cell parameters) with observed peak locations. From this analysis, it was also possible to identify the sample orientation on the substrate.
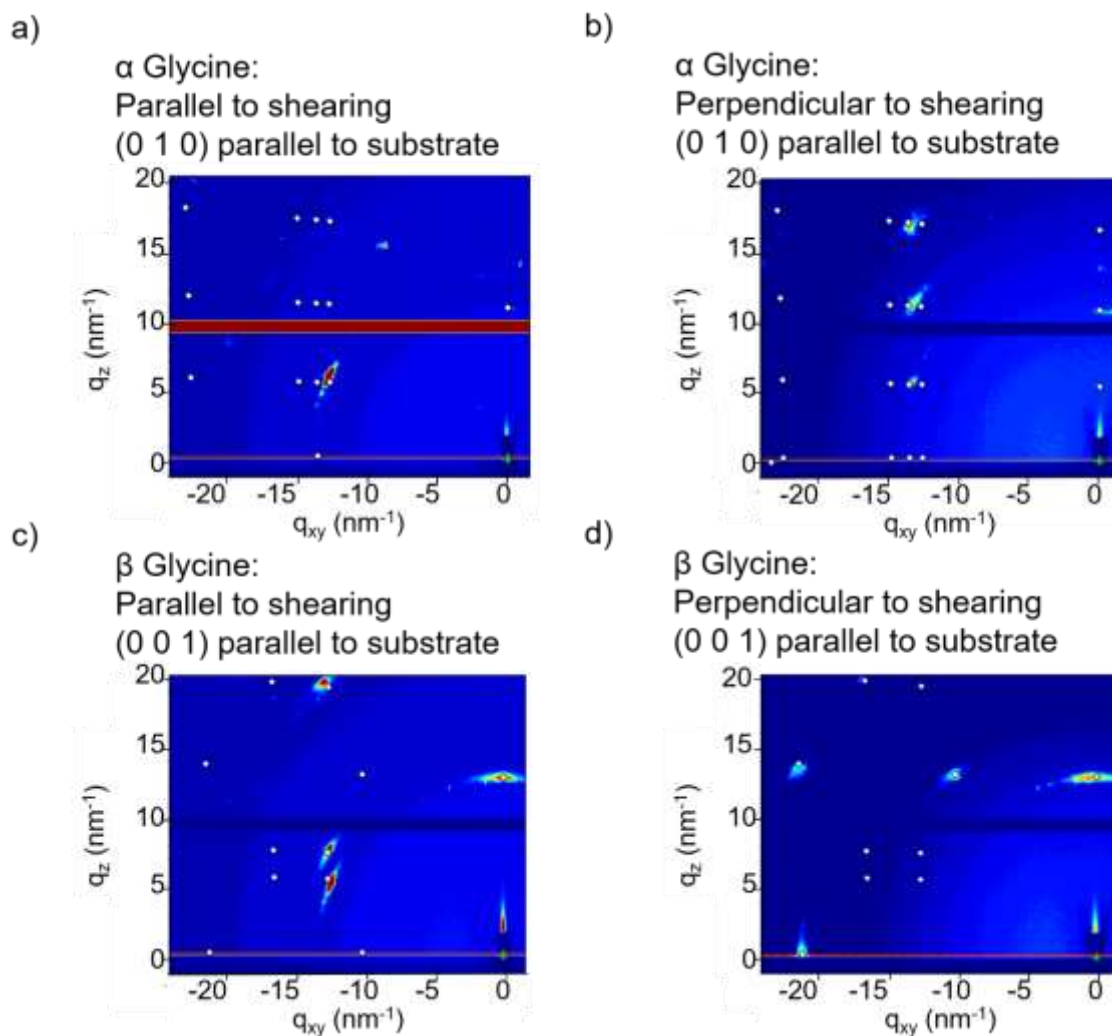
Figure 16. GIXD and corresponding integration patterns obtained for a), b) α glycine, c), d) β glycine Notice the difference in peak intensity as the samples are rotated for highly aligned glycine samples. Sample alignment biases the peak intensity, accounting for differences between experimental and simulated PXRD data.

Figure 16a shows the indexing obtained by matching α glycine unit cell parameters with the GIXD pattern and similarly, figure 16b obtained from matching β parameters.[40, 43] This shows that α glycine was formed with preferential (0 1 0) orientation on the substrate. We also isolated the β form of glycine with (0 0 1) orientation.
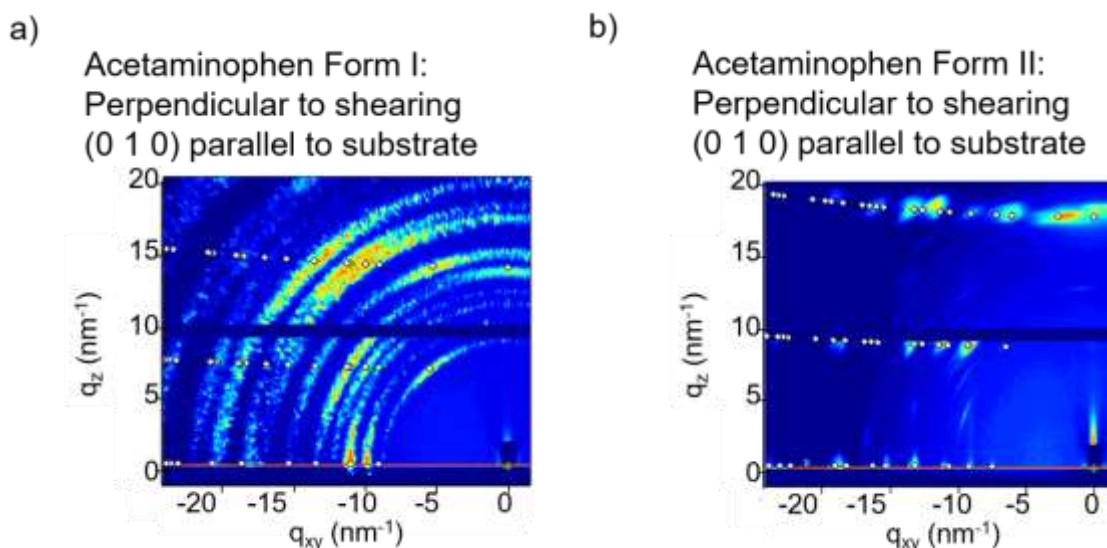

Figure 17. GIXD and corresponding integration patterns obtained for a) acetaminophen Form I and b) acetaminophen Form II. Both forms crystallized with the (0 1 0) plane parallel to the substrate. GIXD peaks in Form I are dispersed due to the sample having more powdery character. Only perpendicular orientation is shown for

For acetaminophen, indexing shows that Form I and Form II were both obtained and crystallized with the (0 1 0) plane parallel to the substrate (figure 17).[41-42] For increased ease of analysis, the diffraction images were integrated along constant radii to obtain powder patterns that could be easily compared to diffraction patterns simulated from crystal structures. The integrated GIXD was compared directly to the reported powder patterns. The peak positions are identical to previously obtained polymorphs for the APIs (Figure 18). For glycine, the α (more stable) and β (less stable) phases were obtained, and the γ (equilibrium) polymorph was not isolated in this study. For acetaminophen, form I (monoclinic, equilibrium) and form II (orthorhombic, metastable) polymorphs were obtained. It was also observed that the amorphous phase formed during solution shearing of acetaminophen crystallized as form II consistently.
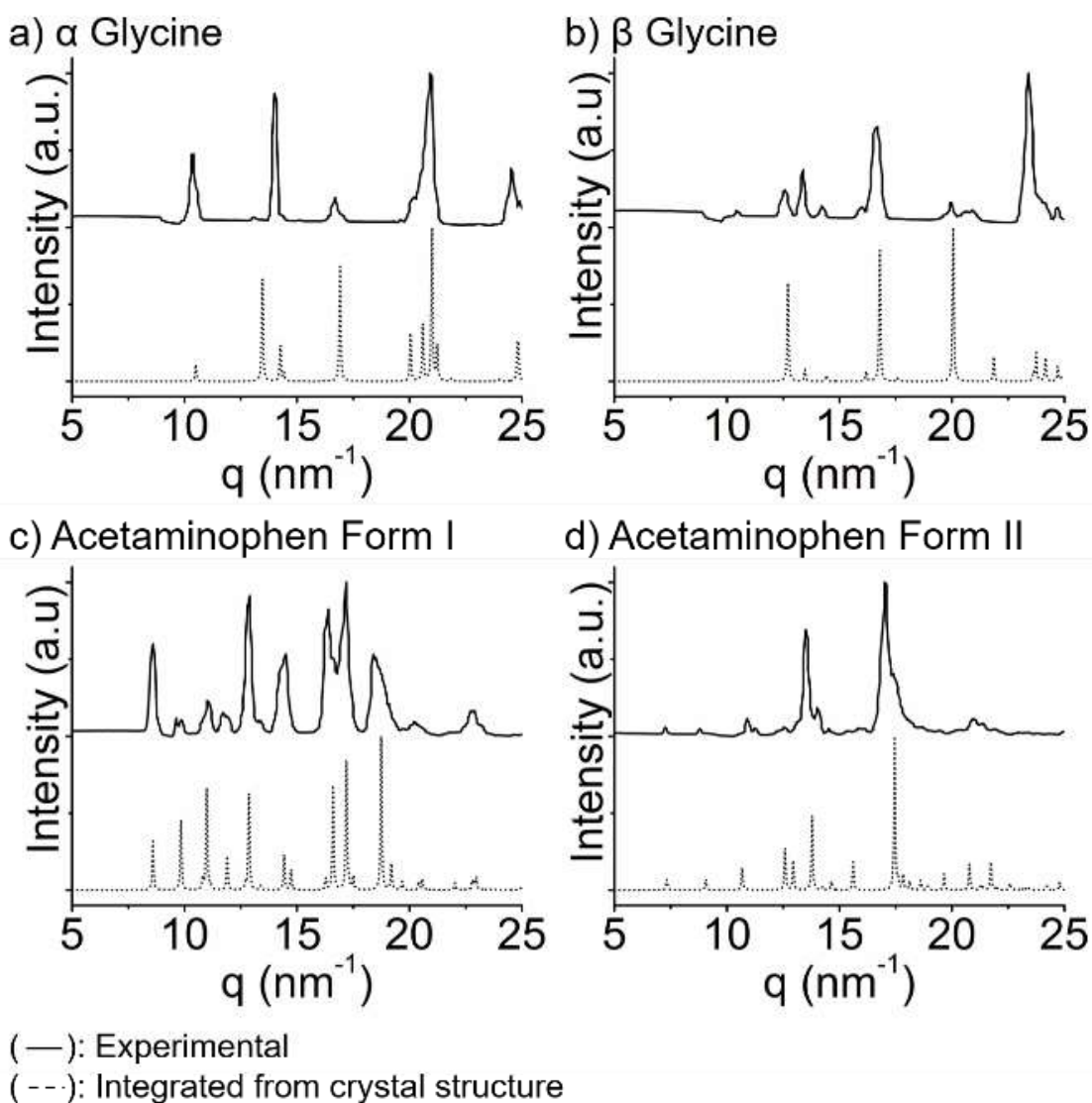
Figure 18. Representative scans obtained from integrating 2-D grazing incidence X-ray diffraction (GIXD) patterns. Dashed patterns are literature reported data a) α glycine formed at 70°C, 0.03 mm s-1, b) β glycine formed at 80°C and 0.11 mm s-1, c) acetaminophen form I formed at 100°C, 0.03 mm s-1, d) acetaminophen form II formed at 100°C and 0.5 mm s^{-1}

With the tools of GIXD and the corresponding integrated patterns, it became clear that using solution shearing, it is possible to isolate different polymorphs for both molecules. It became a focus to form an understanding of the factors that contribute to isolation of polymorphs. The samples were characterized for polymorphism and then organized according to sample processing conditions (shearing speed and temperature). The transformation boundary – where the polymorph selection changes – was studied in more detail through repeated sampling at these conditions, for a total of 65 samples collected for glycine

and 79 samples collected for acetaminophen. Assembling processing diagrams (Figure 19) show that pure phases are isolated at the slowest and fastest shearing speeds, with intermediate speeds producing both polymorphs.

Figure 19: Processing diagrams for a) glycine and b) acetaminophen as a function of solution shearing speed and temperature. Polymorph selection is influenced by the solution shearing speed. Column graphs indicate the relative occurrence of each polymorph in the films. Summation of the bar graphs over 1 for any condition indicates film formation with multiple polymorphs in one sample.

Glycine thin films had a tendency to form as pure α or β polymorph. A relationship between the crystal morphology and polymorph seemed to exist; large crystalline domains were preferentially composed of the α polymorph, while needle-like crystals were preferentially composed of the β polymorph. No interconversion occurred during solution shearing. However, due to variability in the solution shearing process, both polymorphs could be obtained at certain conditions that describe the transformation boundary.

For acetaminophen, the pure polymorphic films were isolated at conditions characterized by fast and slow shearing speeds. The amorphous films formed by solution shearing at faster speeds consistently crystallized as the form II polymorph, while the acetaminophen films solution sheared at lower speeds crystallized as the form I polymorph. However, the intermediate region (characterized by shearing speeds $0.11 - 0.5$ mm s^{-1}) captured a transition between amorphous and crystalline behavior, where films with both forms I and II were observed. More frequently than with glycine, acetaminophen films contained both forms in a single film, which is apparent on the processing diagram where the sum of polymorph frequency for both forms is greater than 1.

It is not surprising for both polymorphs to be present in a film when the samples are processed at intermediate conditions, as nucleation is a stochastic process.[46] It is likely that at the transformation boundary, free energies of formation for the metastable form II and the equilibrium form I are similar, giving rise to both polymorphs. For acetaminophen, stability follows as form I > form II > amorphous phase. Therefore, for both molecules, thinner films, formed at the faster shearing speeds, crystallize as the less stable polymorph. (Figure 19b,c).

Table 1 summarizes the polymorphism and film thickness trends that were observed. This result supports the hypothesis that the one-dimensional confinement of the film thickness during solution shearing is responsible for the stabilization of metastable polymorphs.[32] It is also important to note that

Molecule	Polymorph	Stability	Film Thickness
	γ	Equilibrium	n/a
Glycine	α	More stable	Thick
	β	Least stable	Thin
Acetaminophen	Form I	Equilibrium	Thick
	Form II	Less stable	Thin

Table 1: Observed polymorphism for glycine and acetaminophen with corresponding stabilities. Thick films contained the more stable polymorph.

the transformation boundary for both glycine and acetaminophen occurs at similar temperatures and shearing speeds. This suggests that with the solution shearing technique, one-dimensional confinement play a significant role in directing polymorphism for these two molecules. This is potentially generalizable to a wider set of molecules where the same conditions used in this work could allow for isolation of different polymorphs.

The ability to change processing conditions without changing techniques to create different polymorphs is relevant to the pharmaceutical industry, where it is desirable to screen for the existence of multiple polymorphs quickly. It is convenient that the metastable forms are isolated at faster speeds for both molecules tested. This is ideal both for scaled up processing and high throughput screening for metastable solid phases.

6. Studying the amorphous to crystalline phase transition

As mentioned previously, for some shearing conditions acetaminophen deposited as an amorphous film prior to transforming to the metastable form II polymorph. In preliminary studies, this amorphous behavior was also observed in carbamazepine. Glycine did not deposit as an amorphous film, and this is attributed to a balance between timescales for crystal nucleation and growth being similar to the timescale of film deposition. In molecules where the amorphous phase is observed, the timescale for nucleation is slower than for solid film formation at higher shearing speeds. This mismatch enabled us to isolate the amorphous phase. (Figure 20).

Solution shearing to form thin films thus emerges as a route to study the transient crystallization behavior that is observed. These dynamics provide information about the balance between nucleation and growth. Optical micrographs were captured for the amorphous to crystalline transition in acetaminophen and carbamazepine. Nucleation is designated by the first optical activity (crystal formation) under
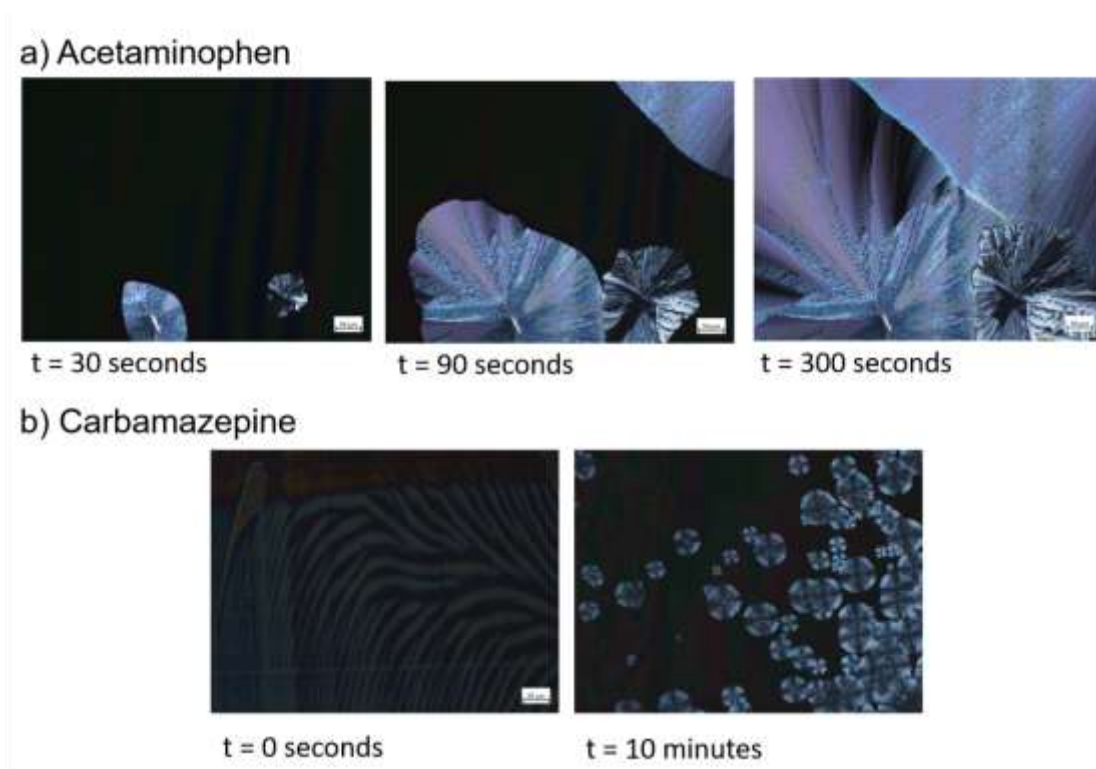

Figure 20: Amorphous to crystalline transition in (a) acetaminophen. (b) Carbamazepine is also shown emphasize that solution shearing has utility in many different molecular systems, however the complete study was not carried out for carbamazepine.

polarized light. Fully crystalline films were marked by the loss of amorphous characteristics under polarized light.

Two types of studies came about through observing the amorphous phase. First, a study tracking the time required to nucleate and fully form a crystalline thin film, which can be summarized as an 'onset of nucleation' curve. Second, after nucleation occurred, the crystal growth rate was observed. For both of these studies, change of the thin films from an amorphous to a crystalline phase was observed using microscopy to detect crystals and to observe the growth. Images were taken at discrete time points, and processed to extract crystal growth rates.

6.1 Solid-state transformation diagram

The transient crystallization dynamics of acetaminophen were studied to construct a solid-state transformation diagram (Figure 21) based on the shearing speed. The operating lines specify the beginning of the solid-state change from amorphous to crystalline (marked by the first optical activity under polarized light), and the end of the solid-state phase change (signified by a fully crystalline thin film).
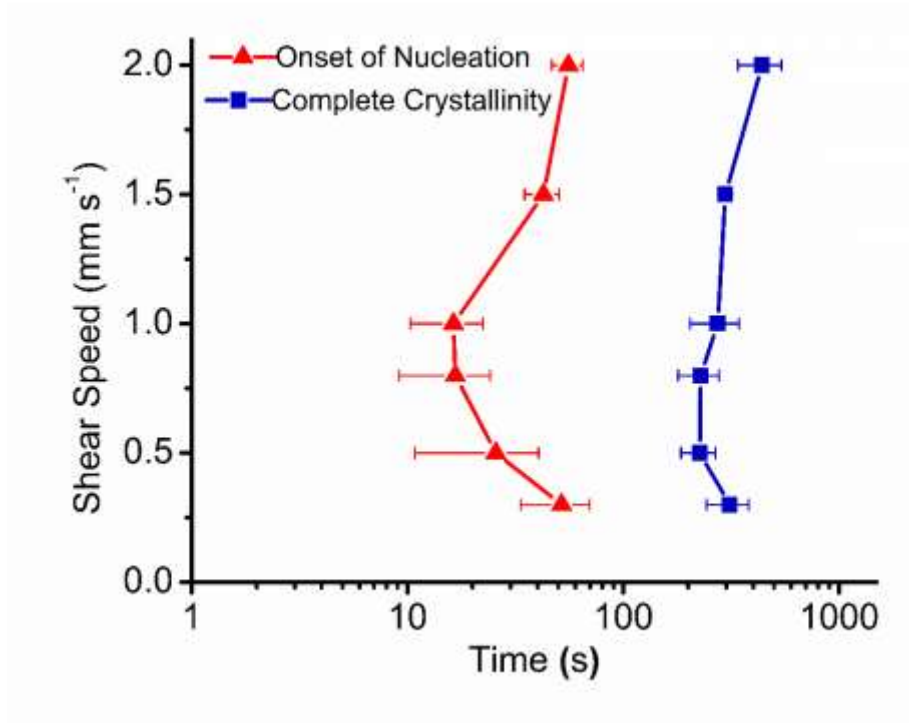

Figure 21. Transformation diagram showing how blade speed relates to the timescale of nucleation and overall crystallization for acetaminophen thin films sheared at 90˚C.

Analogies to a time temperature transformation (TTT) diagram become apparent from observing the shape of the solid-state transformation crystallization diagram. Commonly used in metal and polymer melt systems, a TTT diagram is used to describe the solid-state phase transformations that occur by changing the processing temperature.[47] The resulting phase composition and microstructure of materials is often embedded in the diagram, making it useful to for understanding the link between processing conditions and polymorphism or microstructural change.[47]
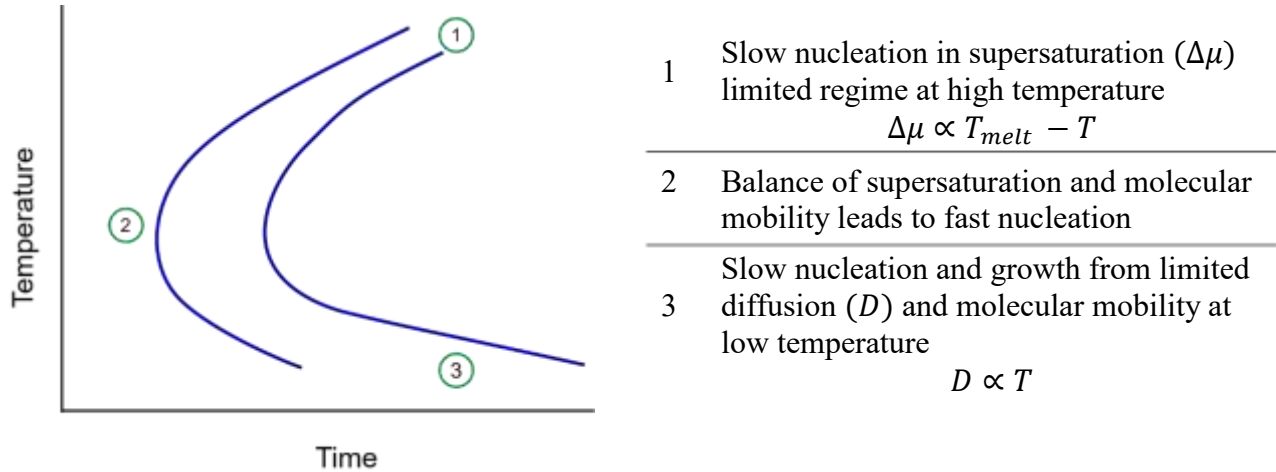

1	Slow nucleation in supersaturation ($\Delta\mu$) limited regime at high temperature $$\Delta\mu \propto T_{melt} - T$$
2	Balance of supersaturation and molecular mobility leads to fast nucleation
3	Slow nucleation and growth from limited diffusion (D) and molecular mobility at low temperature $$D \propto T$$

Figure 22. General shape of a time temperature transformation diagram (TTT) with features (1, 2, 3) marking significant points for nucleation and growth. Fundamentally, the balance between nucleation and growth creates the characteristic curved shape.

While the mechanisms of transformation are well understood for a TTT (Figure 22), it is unclear what directs the nucleation and growth rates in the solution shearing system. As a preliminary hypothesis, it is possible that the mechanism of growth is different in the thick films, formed under a slow blade speed, compared to the thinner films formed using a fast blade speed.

Guiding us towards understanding, we will incorporate the Avrami equation (equation 3), which characterizes the extent of transformation (y) of one solid phase to another as a function of time (t).[48]

$$y = 1 - exp\left(\frac{t}{\tau}\right)^{m} \tag{3}$$

Here, τ is a time constant that describes the process growth time (with a strong volumetric dependence), and m describes the dimensionality of growth. In thinner films, where confinement is more significant, growth will occur in two dimensions ($m = 2$) while in thicker films there is more opportunity for growth

to occur in three dimensions, increasing the value of the exponential factor. This is where there is potential for a change in the mechanism for growth. However, this does not completely describe the transformations observed here and the Avrami parameters have not yet been determined in this system.

Understanding and controlling solid-state phase transformations can be utilized to study the balance between molecular mobility, nucleation and growth, as well as study the relative phase stability. The transformation diagrams obtained through solution shearing can also provide insight about the crystallization kinetics, similar to how a time temperature transformation diagram is used for undercooled melt systems.

6.2 Determining crystal growth rate

In this study, thin films were formed at constant temperature with varying shear speed to produce thin films with differing thickness. Calculating the crystal growth rate from optical images required more precise image processing techniques, which were carried out using ImageJ, with an end goal of extracting the radial growth rate of the amorphous to crystalline transformation (figure 23).
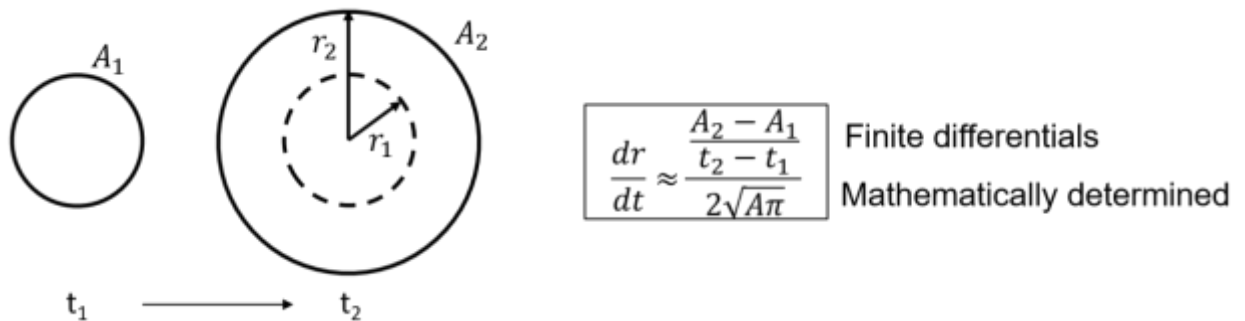
Figure 23. Theoretical derivation of growth rate and labeled schematic of a growing crystal. The A in the denominator is approximated as A_2.

A linear, radial growth rate dr/dt can be determined beginning with an expression for crystal area (4) and the corresponding expression for radius (5). The following derivations were carried out with the assumption that the crystal shape is similar to a circle.

$$A = \pi r^2 \tag{4}$$

$$dA = 2\pi r \, dr = 2\pi \sqrt{\frac{A}{\pi}} \, dr \tag{5}$$

41

The area growth rate is a function that is composed of the area change with radius and the radius change with time dr/dt, the value we are actually concerned with

$$\frac{dA}{dt} = \frac{dA}{dr}\frac{dr}{dt} \tag{6}$$

Through rearrangement of (6) and substituting (5) an expression for dr/dt emerges (7)

$$\frac{dr}{dt} = \frac{\frac{dA}{dt}}{2\sqrt{A\pi}} \tag{7}$$

Finally, the dA/dt term is approximated from finite differentials, with values for change in area $(A_2 - A_1)$ found using image processing at controlled time points $(t_2 - t_1)$.

$$\frac{dr}{dt} = \frac{\frac{A_2 - A_1}{t_2 - t_1}}{2\sqrt{A\pi}} \tag{8}$$

An example of this process for acetaminophen is shown in figure 24. Throughout the period of observation (up to 15 minutes of observation), the growth rate is constant. This indicates that it is not necessary to calculate the growth rate at many different times. Instead, it is suitable to complete the
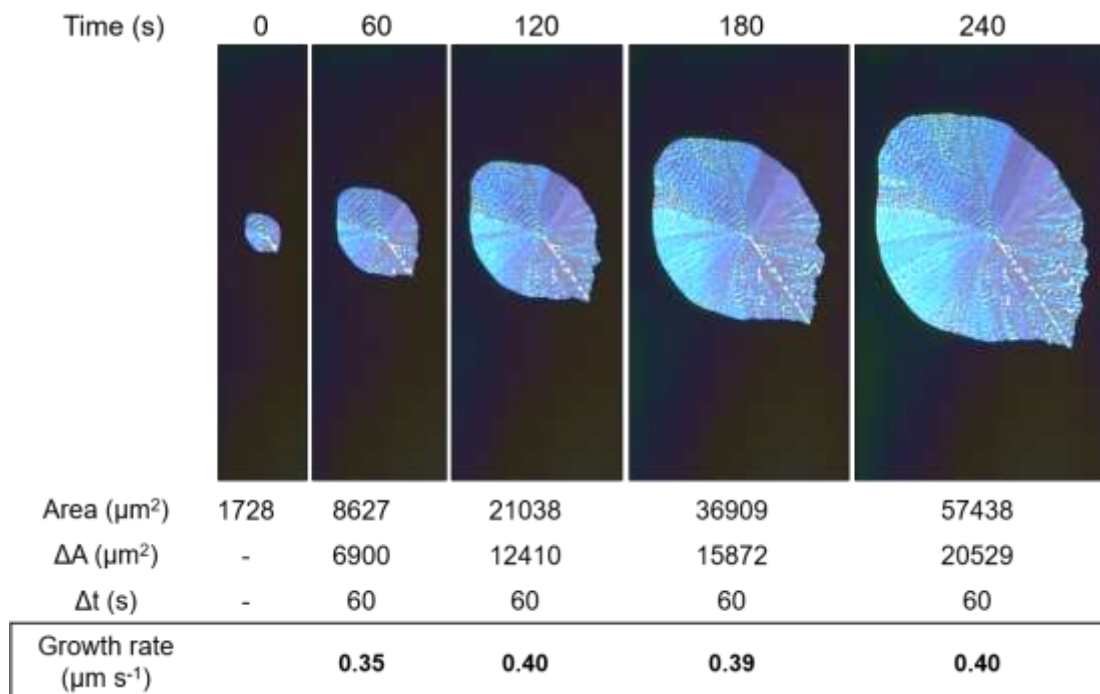
| Time (s)	0	60	120	180	240
Area (μm^2)	1728	8627	21038	36909	57438
ΔA (μm^2)	-	6900	12410	15872	20529
Δt (s)	-	60	60	60	60
Growth rate ($\mu m\ s^{-1}$)		0.35	0.40	0.39	0.40

Figure 24: example of growth rate calculation for a film processed at 80 degrees, 0.3 mm/s, showing a relatively stable growth rate calculated over the time period of 4 minutes.

calculation once or twice for each sample. It would be more meaningful to repeat samples at the same condition to see if sample to sample variation is significant.

General results for experiments at 80 ˚C and 90 ˚C are presented in table 2. From the current data set, it is not reasonable to draw generalizations about how growth rate might change with processing conditions. However, expanding this work will give insight to how growth might be influenced by confinement in a thin film. This will contribute to describing the mechanisms of growth for the solid-state transformation diagram, specifically in the biphasic region.

Temperature (˚C)	Shearing Speed (mm s^{-1})	Average growth rate (standard deviation) (μm s^{-1})	Usable samples/total samples
80	0.3	0.58 (0.39)	3/3
80	0.5	0.40 (0.28)	2/3
80	1	n/a	0/1
90	0.3	0.74 (0.16)	3/4
90	0.5	0.63 (0.14)	3/5
90	1	n/a	0/1

Table 2: Growth rates for films formed at 80 ˚C and 90˚C. Shearing blade speeds ranged from 0.3 -1 mm s^{-1},.

Moving forward, there are some anticipated barriers in describing the growth accurately, both with the assumptions made and with the data processing method. The assumption that the crystal shape can be approximate as a circle is generally valid to providing information about crystal size change. However, obtaining more accurate growth information can be obtained using other shape assumptions. Using the area given from ImageJ, the next step requires extracting a radius (or characteristic lengths for other shapes).

For a particular shape, the ratio of area to perimeter ($R_{A/P}$) is calculable and can be used as a shape factor that describes the potential crystal shapes. An approximation of the error associated with assuming different crystal shapes (analyzed in table 3) shows that there could be up to 13% error when comparing the theoretical shape factor ($R_{A/P}$) and the actual shape factor obtained by dividing the area and perimeter values obtained from ImageJ case. For example, when assuming the crystal analyzed in table 3 is a rhombus with internal angles of 80 and 100˚, the shape factor ($R_{A/P}$) is 29.9 μm, calculated using the area of the crystal obtained from ImageJ. With the actual shape having a shape factor of 30.04

μm (area of 6210 μm² and a perimeter of 316 μm), the error associated with the rhombus assumption is -0.2% compared to 13% for the assumption of a circle.

|	Circle	Triangle	Square Rhombus ($\theta = 90°$, $90°$)	Rhombus ($\theta = 80°$, $100°$)	Rhombus ($\theta = 70°$, $110°$)
Variable definitions					
$R_{A/P}(A)$	$\dfrac{\sqrt{A/\pi}}{2}$	$0.144\sqrt{\dfrac{4A}{\sqrt{3}}}$	$\dfrac{\sqrt{A}}{4}$	$\dfrac{\sqrt{Asin\theta}}{4}$	$\dfrac{\sqrt{Asin\theta}}{4}$
Calculated $R_{A/P}(A)$*	34.1	26.4	30.2	29.9	29.3
Error	13%	-12%	1%	-0.2%	-3%
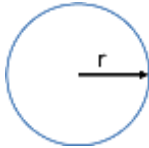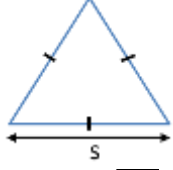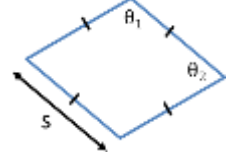
Table 3: example of growth rate calculation for a film processed at 80 degrees, 0.3 mm/s, showing a relatively stable growth rate calculated over the time period of 4 minutes.
*Calculations completed for a trial where A = 6210 μm² and P = 316 μm (R actual = 30.04 μm)

The choice of a circle simplifies the calculation compared to a more accurate shape selection, like a rhombus, where two primary axes define the shape rather than one radius. Further, there is some variation in the shape of the growing crystal and it is unclear what the driving force for shape evolution throughout growth is (a crystal that begins circular may undergo fast growth in one direction, thus convoluting the shape).

On obstacle that has been encountered is with our ability to resolve growing crystals using the ImageJ analysis method. Shown in figure 25 there are several cases in which the area and perimeter cannot be accurately specified using ImageJ.
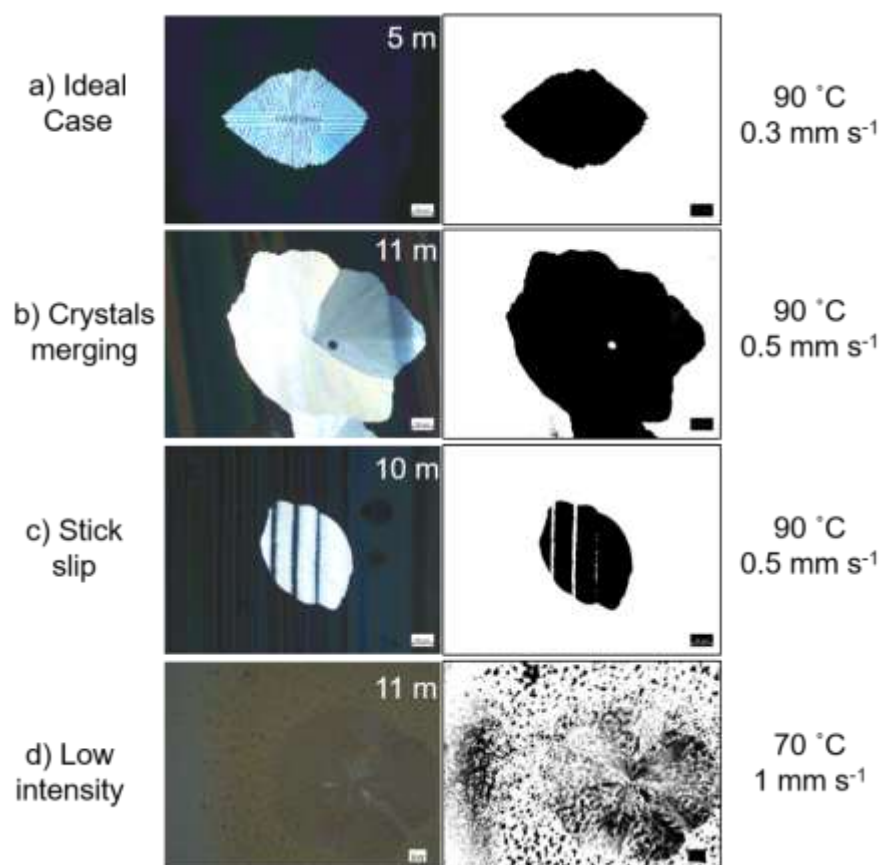
Figure 25: a) An ideal case of crystallization, where ImageJ can accurately detect the crystal. b) an example of two crystals merging and skewing the measurement. c) Stick slip during the shearing process creates patterns in the crystal that makes the crystal discontinuous. d) Thin films have low intensity crystal formation that cannot be distinguished form the background

Crystals growing together can make it difficult to correctly report the crystal area. Merging crystals cannot be avoided, but this indicates that if the growth rates are stable with time, then any two images can be used. Two images can be used that take place before merging occurs. Stick slip patterns in the film are sometimes created as an artifact of the shearing process, where fluid dynamics and meniscus instability can create regions of variable thickness.[45] This presents as lines, shown in figure 25c. ImageJ cannot accurately perform the thresholding function for these crystals. An improved shearing setup was assembled, where the stick slip motion is less prominent.

Finally, in the thinner films (formed at low temperatures or fast shearing speeds), the amorphous background and the polarized crystal are not significantly different. Therefore, the crystal is not

detectable. The low intensity samples can be manually outlined and counted, however this is inefficient. lowers the throughput of analysis, and introduces human error.

The dynamics of crystallization are of general interest. The solution shearing technique is a simple and straightforward method to obtain the amorphous phase of some APIs, which is of interest because amorphous phases have rapid dissolution dynamics. Further, this technique has utility in obtaining the amorphous phase at elevated temperatures. Normally, the amorphous phase is highly prone to undergoing transformations and is typically controlled using careful temperature control, humidity control, or inclusion of materials (like polymers) that inhibit crystallinity.

7. Conclusion and continuation of work.

7.1 Conclusion

Solution shearing is an effective tool to sample processing conditions rapidly while utilizing a small amount of material, and is a robust method to isolate equilibrium and metastable polymorphs, as demonstrated in organic semiconductors. This work broadens the relevance of solution shearing to include pharmaceuticals. In this study, we show that controlling the shearing speed and temperature allows us to obtain polymorphic phases in glycine and acetaminophen with metastable polymorphs being present in the thinnest films (figure 26). We hypothesize that confinement is responsible for stabilization of metastable polymorphs. Previous studies have demonstrated that shearing induces polymorphism due to one-dimensional confinement. The observed solid-state phase formation of a molecule using solution shearing is highly dependent on the molecular structure, but solution shearing is capable of isolating the amorphous phase in multiple candidate APIs, even those suffering from low aqueous solubility. Moving forward, solution shearing can be adopted as a method to aid in polymorph screening and selection during drug development, with the processing diagrams provided as a starting point to obtain metastable polymorphs. Future studies with this technology will study the utility of solution shearing to produce tunable solubility.
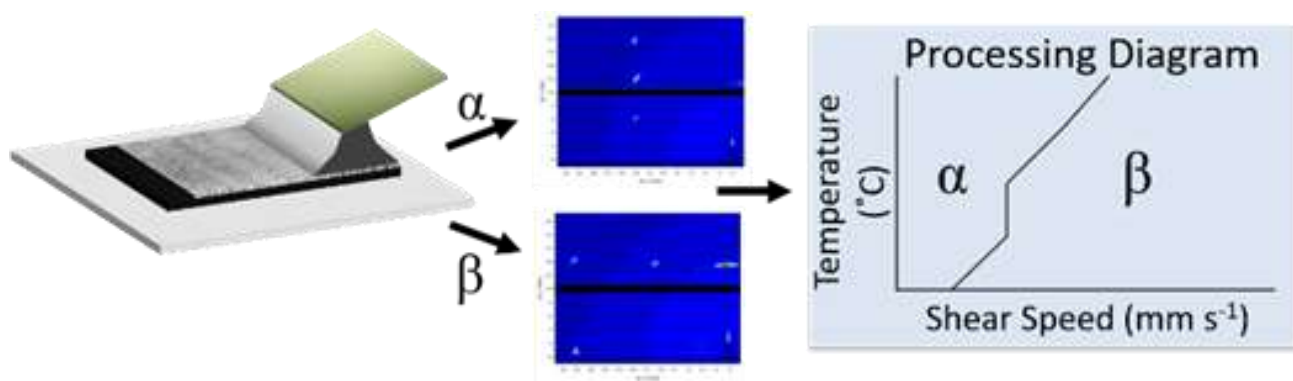

Figure 26. Schematic description of solution shearing being used to isolate polymorphs, as outlined in this study.

7.2 Future work

1. In this work, film formation was described and the mechanisms of deposition were discussed using film thickness as the primary evidence for the molecular assembly process. Here, we propose to study solution shearing through in-situ optical microscopy. The shearing setup has been interfaced with an optical microscope and high-speed camera. Using this, the film formation can be specified in terms of observed molecular attachment. Growth of crystals as evaporation occurs can be observed in order to understand more about why a particular shape is selected for growth. Using this technique, we approach the answer to questions like why does glycine begin to form different shaped crystallites at different shearing speeds?

2. This work focused on two specific examples of model drug molecules. Model systems are easy to study because they are well characterized and behave in predictable ways. It is interesting to explore when the solution shearing technique might break-down from ideal cases. The technique will next be applied to caffeine and carbamazepine. Carbamazepine is of particular interest because it has low aqueous solubility and thus could benefit from isolation of metastable forms with increased dissolution properties. Small proteins will also be studied, where crystallization is an active area of research.

3. The kinetics of crystallization studies are still being fully developed, however the framework for gaining understanding are developed. The objective is to create a full picture of growth rates and kinetics of crystallization. This will expand the temperature and shearing speed conditions sampled with more refinement to construct improved kinetic crystallization diagrams. Growth rate studies will be continued to understand the shape of the curves on transformation boundary of the amorphous/crystalline transition.

4. The driver of this type of work is to obtain polymorphs with enhanced dissolution properties. Moving forward, solubility studies will be incorporated with the thin films, either in a bulk solubility test or through interfacing a fluidic flow system. This will quantify the performance of solution shearing for pharmaceutical systems more fully.

8. References

1. Khanna, I., Drug discovery in pharmaceutical industry: productivity challenges and trends. *Drug Discov Today* **2012,** *17* (19), 1088-1102.

2. Woodcock, J.; Woosley, R., The FDA Critical Path Initiative and Its Influence on New Drug Development. *Annu. Rev. Med.* **2008,** *59* (1), 1-12.

3. Dwyer, L.; Kulkarni, S.; Ruelas, L.; Myerson, A., Two-Stage Crystallizer Design for High Loading of Poorly Water-Soluble Pharmaceuticals in Porous Silica Matrices. *Crystals* **2017,** *7* (5), 131.

4. Kalepu, S.; Nekkanti, V., Insoluble drug delivery strategies: review of recent advances and business prospects. *Acta Pharm Sin B* **2015,** *5* (5), 442-453.

5. Newman, A. W.; Byrn, S. R., Solid-state analysis of the active pharmaceutical ingredient in drug products. *Drug Discov Today* **2003,** *8* (19), 898-905.

6. Allen, T. M.; Cullis, P. R., Drug Delivery Systems: Entering the Mainstream. *Science* **2004,** *303* (5665), 1818-1822.

7. Fahr, A.; Liu, X., Drug delivery strategies for poorly water-soluble drugs. *Expert Opin. Drug Deliv.* **2007,** *4* (4), 403-416.

8. Kim, J.-W.; Shim, H.-M.; Lee, J.-E.; Koo, K.-K., Interfacial Effect of Water/Oleic Acid Emulsion on Polymorphic Selection in the Cooling Crystallization of Glycine. *Cryst. Growth. Des.* **2012,** *12* (10), 4739-4744.

9. Brittain, H., Thermodynamic vs. kinetic solubility: knowing which is which. *Am Pharmaceut Rev* **2014,** *17* (3), 10-6.

10. Hilfiker, R.; Blatter, F.; Raumer, M. v., Relevance of Solid-state Properties for Pharmaceutical Products. In *Polymorphism*, Wiley-VCH Verlag GmbH & Co. KGaA: 2006; pp 1-19.

11. Nývlt, J., The Ostwald Rule of Stages. *Crystal Research and Technology* **1995,** *30* (4), 443-449.

12.   Morissette, S. L.; Almarsson, Ö.; Peterson, M. L.; Remenar, J. F.; Read, M. J.; Lemmo, A. V.; Ellis, S.; Cima, M. J.; Gardner, C. R., High-throughput crystallization: polymorphs, salts, co-crystals and solvates of pharmaceutical solids. *Adv. Drug Deliv. Rev.* **2004,** *56* (3), 275-300.

13.   Hilfiker, R.; De Paul, S. M.; Szelagiewicz, M., Approaches to Polymorphism Screening. In *Polymorphism*, Wiley-VCH Verlag GmbH & Co. KGaA: 2006; pp 287-308.

14.   Childs, S. L.; Chyall, L. J.; Dunlap, J. T.; Coates, D. A.; Stahly, B. C.; Stahly, G. P., A Metastable Polymorph of Metformin Hydrochloride: Isolation and Characterization Using Capillary Crystallization and Thermal Microscopy Techniques. *Cryst. Growth. Des.* **2004,** *4* (3), 441-449.

15.   Price, S. L., The computational prediction of pharmaceutical crystal structures and polymorphism. *Adv. Drug Deliv. Rev.* **2004,** *56* (3), 301-319.

16.   Lee, E. H., A practical guide to pharmaceutical polymorph screening & selection. *Asian J. Pharm.* **2014,** *9* (4), 163-175.

17.   Leon, R. A. L.; Badruddoza, A. Z. M.; Zheng, L.; Yeap, E. W. Q.; Toldy, A. I.; Wong, K. Y.; Hatton, T. A.; Khan, S. A., Highly Selective, Kinetically Driven Polymorphic Selection in Microfluidic Emulsion-Based Crystallization and Formulation. *Cryst. Growth. Des.* **2015,** *15* (1), 212-218.

18.   Jiang, Q.; Ward, M. D., Crystallization under nanoscale confinement. *Chem. Soc. Rev.* **2014,** *43* (7), 2066-2079.

19.   Hamilton, B. D.; Hillmyer, M. A.; Ward, M. D., Glycine Polymorphism in Nanoscale Crystallization Chambers. *Cryst. Growth. Des.* **2008,** *8* (9), 3368-3375.

20.   Buanz, A. B. M.; Gaisford, S., Formation of Highly Metastable β Glycine by Confinement in Inkjet Printed Droplets. *Cryst. Growth. Des.* **2017,** *17* (3), 1245-1250.

21.   Trauffer, D. I.; Maassel, A. K.; Snyder, R. C., Non-Needle-like Morphology of β-Glycine Particles Formed from Water Solutions via Monodisperse Droplet Evaporation. *Cryst. Growth. Des.* **2016,** *16* (4), 1917-1922.

22.   Lee, S.; Feldman, J.; Lee, S. S., Nanoconfined Crystallization of MAPbI3 to Probe Crystal Evolution and Stability. *Cryst. Growth. Des.* **2016,** *16* (8), 4744-4751.

23.   Burcham, C.; Jarmer, D., *Industrial Crystallization of Pharmaceuticals: Capability Requirements to Support an Outsourcing Paradigm*. 2013; Vol. 14.

24.   Giulietti, M.; Seckler, M. M.; Derenzo, S.; Ré, M. I.; Cekinski, E., Industrial Crystallization and Precipitation from Solutions: State of the Technique. *Brazilian Journal of Chemical Engineering* **2001,** *18*, 423-440.

25.   Giri, G.; Verploegen, E.; Mannsfeld, S. C. B.; Atahan-Evrenk, S.; Kim, D. H.; Lee, S. Y.; Becerril, H. A.; Aspuru-Guzik, A.; Toney, M. F.; Bao, Z., Tuning charge transport in solution-sheared organic semiconductors using lattice strain. *Nature* **2011,** *480* (7378), 504-508.

26.   Ahn, S.; Matzger, A. J., Six Different Assemblies from One Building Block: Two-Dimensional Crystallization of an Amide Amphiphile. *J. Am. Chem. Soc.* **2010,** *132* (32), 11364-11371.

27.   Erdemir, D.; Lee, A. Y.; Myerson, A. S., Nucleation of Crystals from Solution: Classical and Two-Step Models. *Acc. Chem. Res.* **2009,** *42* (5), 621-629.

28.   Threlfall, T., Crystallisation of Polymorphs: Thermodynamic Insight into the Role of Solvent. *Organic Process Research & Development* **2000,** *4* (5), 384-390.

29.   Gu, C.-H.; Young, V.; Grant, D. J. W., Polymorph screening: Influence of solvents on the rate of solvent-mediated polymorphic transformation. *J. Pharm. Sci.* **2001,** *90* (11), 1878-1890.

30.   Becerril, H. A.; Roberts, M. E.; Liu, Z.; Locklin, J.; Bao, Z., High-Performance Organic Thin-Film Transistors through Solution-Sheared Deposition of Small-Molecule Organic Semiconductors. *Adv. Mater.* **2008,** *20* (13), 2588-2594.

31.   Gu, X.; Zhou, Y.; Gu, K.; Kurosawa, T.; Guo, Y.; Li, Y.; Lin, H.; Schroeder, B. C.; Yan, H.; Molina-Lopez, F.; Tassone, C. J.; Wang, C.; Mannsfeld, S. C. B.; Yan, H.; Zhao, D.; Toney, M. F.; Bao, Z., Roll-to-Roll Printed Large-Area All-Polymer Solar Cells with 5% Efficiency Based on a Low Crystallinity Conjugated Polymer Blend. *Advanced Energy Materials* **2017,** *7* (14), 1602742-n/a.

32. Giri, G.; Li, R.; Smilgies, D.-M.; Li, E. Q.; Diao, Y.; Lenn, K. M.; Chiu, M.; Lin, D. W.; Allen, R.; Reinspach, J.; Mannsfeld, S. C. B.; Thoroddsen, S. T.; Clancy, P.; Bao, Z.; Amassian, A., One-dimensional self-confinement promotes polymorph selection in large-area organic semiconductor thin films. *Nature Communications* **2014,** *5*, 3573.

33. Lee, A. Y.; Lee, I. S.; Myerson, A. S., Factors Affecting the Polymorphic Outcome of Glycine Crystals Constrained on Patterned Substrates. *Chemical Engineering & Technology* **2006,** *29* (2), 281-285.

34. Beyer, T.; Day, G. M.; Price, S. L., The Prediction, Morphology, and Mechanical Properties of the Polymorphs of Paracetamol. *J. Am. Chem. Soc.* **2001,** *123* (21), 5086-5094.

35. Peterson, M. L.; McIlroy, D.; Shaw, P.; Mustonen, J. P.; Oliveira, M.; Almarsson, Ö., Crystallization and Transformation of Acetaminophen Trihydrate. *Cryst. Growth. Des.* **2003,** *3* (5), 761-765.

36. Dawson, A.; Allan, D. R.; Belmonte, S. A.; Clark, S. J.; David, W. I. F.; McGregor, P. A.; Parsons, S.; Pulham, C. R.; Sawyer, L., Effect of High Pressure on the Crystal Structures of Polymorphs of Glycine. *Cryst. Growth. Des.* **2005,** *5* (4), 1415-1427.

37. Widjonarko, N., Introduction to Advanced X-ray Diffraction Techniques for Polymeric Thin Films. *Coatings* **2016,** *6* (4), 54.

38. Smilgies, D.-M.; Blasini, D. R., Indexation scheme for oriented molecular thin films studied with grazing-incidence reciprocal-space mapping. *J. Appl. Crystallogr.* **2007,** *40* (4), 716-718.

39. Hammersley, A., FIT2D: a multi-purpose data reduction, analysis and visualization program. *J. Appl. Crystallogr.* **2016,** *49* (2), 646-652.

40. Marsh, R., A refinement of the crystal structure of glycine. *Acta Crystallogr.* **1958,** *11* (9), 654-663.

41. Haisa, M.; Kashino, S.; Kawai, R.; Maeda, H., The Monoclinic Form of p-Hydroxyacetanilide. *Acta Crystallogr. Sect. B* **1976,** *32* (4), 1283-1285.

42.   Thomas, L. H.; Wales, C.; Zhao, L.; Wilson, C. C., Paracetamol Form II: An Elusive Polymorph through Facile Multicomponent Crystallization Routes. *Cryst. Growth. Des.* **2011,** *11* (5), 1450-1452.

43.   Iitaka, Y., The crystal structure of [beta]-glycine. *Acta Crystallogr.* **1960,** *13* (1), 35-45.

44.   Le Berre, M.; Chen, Y.; Baigl, D., From Convective Assembly to Landau−Levich Deposition of Multilayered Phospholipid Films of Controlled Thickness. *Langmuir* **2009,** *25* (5), 2554-2557.

45.   Aranson, I. S.; Tsimring, L. S.; Vinokur, V. M., Stick-slip friction and nucleation dynamics of ultrathin liquid films. *Phys. Rev. B* **2002,** *65* (12), 125402.

46.   Goh, L.; Chen, K.; Bhamidi, V.; He, G.; Kee, N. C. S.; Kenis, P. J. A.; Zukoski, C. F.; Braatz, R. D., A Stochastic Model for Nucleation Kinetics Determination in Droplet-Based Microfluidic Systems. *Cryst. Growth. Des.* **2010,** *10* (6), 2515-2521.

47.   Yu, L.; Davidson, E.; Sharma, A.; Andersson, M. R.; Segalman, R.; Müller, C., Isothermal Crystallization Kinetics and Time–Temperature–Transformation of the Conjugated Polymer: Poly(3-(2′-ethyl)hexylthiophene). *Chem. Mater.* **2017,** *29* (13), 5654-5662.

48.   Avrami, M., Granulation, Phase Change, and Microstructure Kinetics of Phase Change. III. *The Journal of Chemical Physics* **1941,** *9* (2), 177-184.